# Extreme Compression of Heavy-Ion Beam Pulses: Experiments and Modeling

A. B. Sefkow

Princeton Plasma Physics Laboratory

22nd Particle Accelerator Conference

Albuquerque, NM

June 27th, 2007

*In collaboration with*:

R. C. Davidson, P. C. Efthimion, E. P. Gilson, I. D. Kaganovich (PPPL),
J. E. Coleman, P. K. Roy, P. A. Seidl (LBNL),
J. J. Barnard (LLNL), D. R. Welch (Voss Scientific)
...and the rest of the HIFS-VNL Team...

# Outline

0) MOTIVATION AND ISSUES
- a) Overview
- b) Plasma neutralization-assisted focusing of space-charge-dominated beams

1) LONGITUDINAL COMPRESSION: ACCELERATION GAP EFFECTS
- a) Finite-size gap and voltage waveform
- b) Non-zero initial beam temperature (emittance)
- c) Initial pulse length $t_p$, intended fractional tilt *f*, and initial beam energy
- d) Comparison: theoretical models, particle-in-cell simulation, and experiment

2) TIME-DEPENDENT TRANSVERSE DEFOCUSING EFFECT OF THE ACCELERATION GAP
- a) Description of the effect
- b) The "over-focusing" technique for simultaneous transverse and longitudinal compression

3) SIMULTANEOUS FOCUSING USING A STRONG FINAL-FOCUS SOLENOID
- a) Focal plane aberration due to static magnetic field and beam velocity tilt
- b) Supersonic cathodic-arc plasma injection into the high-field region from the low-field end
- c) Collective excitations during the beam-plasma interaction for $n_b > n_p$

# Outline

0) MOTIVATION AND ISSUES
- a) Overview
- b) Plasma neutralization-assisted focusing of space-charge-dominated beams

1) LONGITUDINAL COMPRESSION: ACCELERATION GAP EFFECTS
- a) Finite-size gap and voltage waveform
- b) Non-zero initial beam temperature (emittance)
- c) Initial pulse length $t_p$, intended fractional tilt *f*, and initial beam energy
- d) Comparison: theoretical models, particle-in-cell simulation, and experiment

2) TIME-DEPENDENT TRANSVERSE DEFOCUSING EFFECT OF THE ACCELERATION GAP
- a) Description of the effect
- b) The “over-focusing” technique for simultaneous transverse and longitudinal compression

3) SIMULTANEOUS FOCUSING USING A STRONG FINAL-FOCUS SOLENOID
- a) Focal plane aberration due to static magnetic field and beam velocity tilt
- b) Supersonic cathodic-arc plasma injection into the high-field region from the low-field end
- c) Collective excitations during the beam-plasma interaction for $n_b > n_p$

Relevant research for many areas:

- Nonneutral plasma physics
  - Theoretical techniques, space-charge effects
- High-energy and nuclear physics
  - Accelerator physics and technology
- High-energy-density plasma physics
  - Warm-dense-matter studies
- Magnetic fusion plasma physics
  - Beam-plasma interaction, diagnostics
- Advanced nonlinear dynamics
  - Chaos, collective processes
- Advanced computing
  - PIC/hybrid approaches, parallel computation

**Example parameters at target:**
*4 GeV beam energy, ~16 beams*

*LONGITUDINAL COMPRESSION:*
*~10 kA / beam, 10 ns pulses*

*TRANSVERSE COMPRESSION:*
*few mm radius*

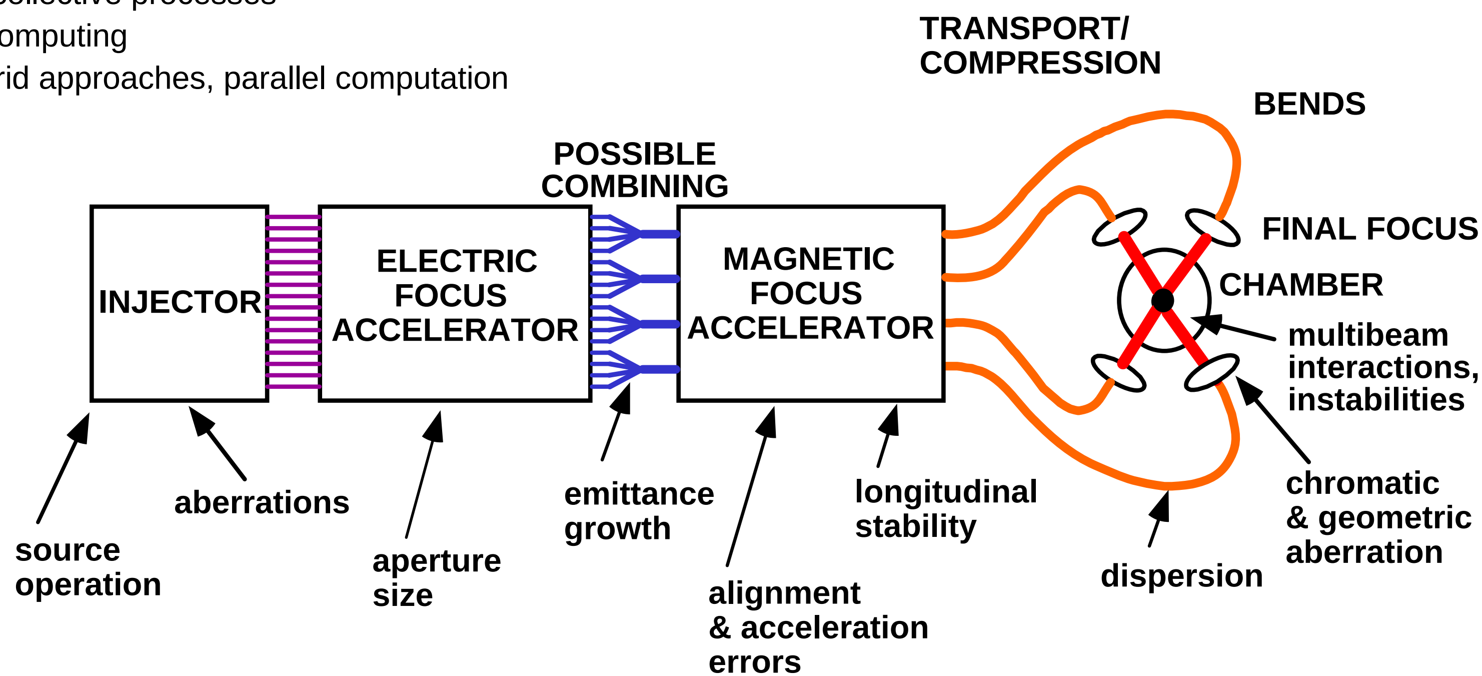

Key scientific issues

- Development of high-current, compact ion sources and injectors
- Accelerate beams to large energies (HIF: GeV) at high intensities and currents (tens of kAs)
- **Transport intense beams and transversely focus to small spot size (< 2 mm)**
- **Longitudinally focus (compress in time) to short pulse widths (< 10 ns)**
- Optimize targets robust to beam aiming errors
- Develop attractive chamber concepts

## Key scientific issues

- Development of high-current, compact ion sources and injectors
- Accelerate beams to large energies (HIF: GeV) at high intensities and currents (tens of kAs)
- **Transport intense beams and transversely focus to small spot size (< 2 mm)**
- **Longitudinally focus (compress in time) to short pulse widths (< 10 ns)**
- Optimize targets robust to beam aiming errors
- Develop attractive chamber concepts

## Key physics issues affecting high-intensity ion beam propagation

- Quality of injected beam
- Emittance growth
- Beam-plasma instabilities
- **Transport and focusing (transverse and longitudinal), and associated aberration**
- **Beam charge and current neutralization effects**
- Ionization of beam and background gas
- Stray electron behavior
- Multiple beam effects

# Outline

0) MOTIVATION AND ISSUES
- a) Overview
- b) Plasma neutralization-assisted focusing of space-charge-dominated beams

1) LONGITUDINAL COMPRESSION: ACCELERATION GAP EFFECTS
- a) Finite-size gap and voltage waveform
- b) Non-zero initial beam temperature (emittance)
- c) Initial pulse length $t_p$, intended fractional tilt *f*, and initial beam energy
- d) Comparison: theoretical models, particle-in-cell simulation, and experiment

2) TIME-DEPENDENT TRANSVERSE DEFOCUSING EFFECT OF THE ACCELERATION GAP
- a) Description of the effect
- b) The “over-focusing” technique for simultaneous transverse and longitudinal compression

3) SIMULTANEOUS FOCUSING USING A STRONG FINAL-FOCUS SOLENOID
- a) Focal plane aberration due to static magnetic field and beam velocity tilt
- b) Supersonic cathodic-arc plasma injection into the high-field region from the low-field end
- c) Collective excitations during the beam-plasma interaction for $n_b > n_p$

Neutralized Transport Experiment (NTX) at LBNL

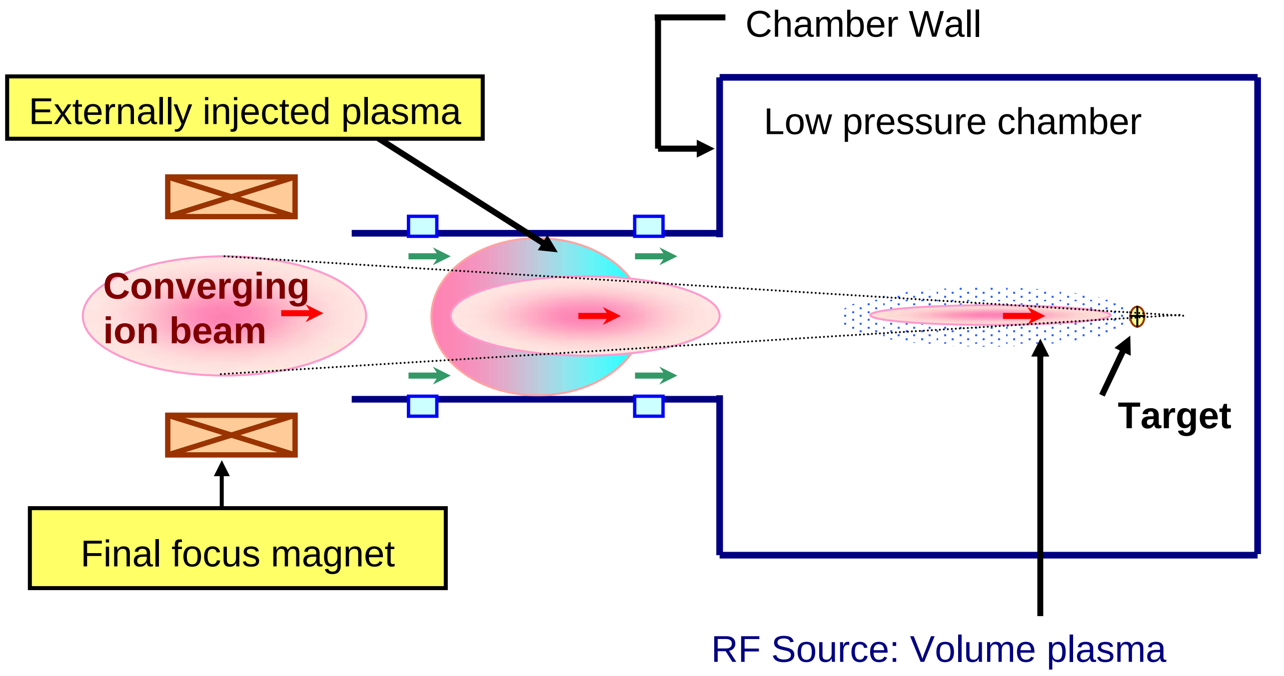


*P. K. Roy, et. al., *Nucl. Instrum. Methods Phys. Res. A* **544**, 225 (2005).
*E. Henestroza, et. al., *Phys. Rev. ST Accel. Beams* **7**, 083501 (2004).
*P. K. Roy, et. al., *Phys. Plasmas* **11**, 2890 (2004).

# Transverse ion beam compression was a success on NTX

**Source range:**
$E_0$ ~ 250-400 keV
$I_0$ ~ 10-80 mA
$r_b$ ~ 1-2 cm
$T_b$ ~ 0.2 eV

Ion species: $K^+$

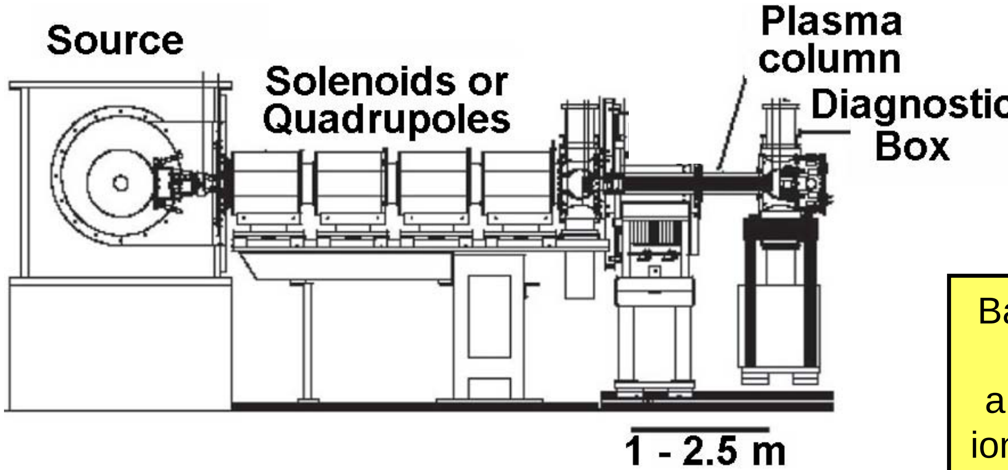


Background neutralizing plasma required to allow quiescent intense ion beam focusing above the space-charge limit

**Source range:**
$E_0$ ~ 250-400 keV
$I_0$ ~ 10-80 mA
$r_b$ ~ 1-2 cm
$T_b$ ~ 0.2 eV

Ion species: $K^+$

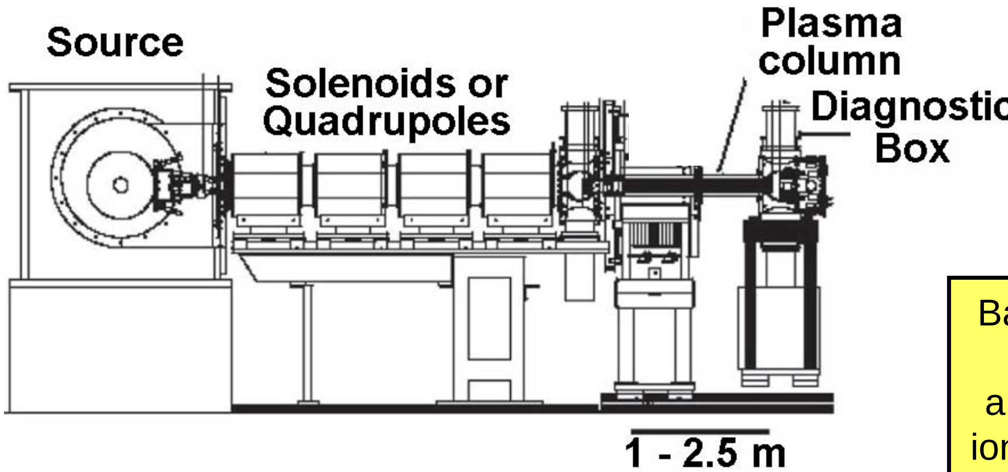


Background neutralizing plasma required to allow quiescent intense ion beam focusing above the space-charge limit

## Experiment

P. K. Roy, *et. al.*, *Nucl. Instrum. Methods Phys. Res. A* **544**, 225 (2005)

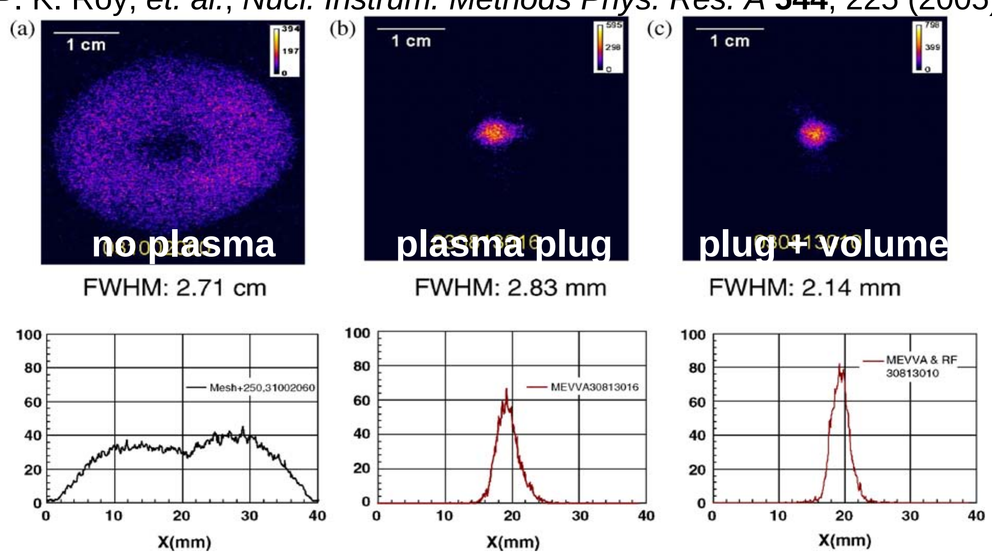

The upgrade of NTX is the Neutralized Drift Compression Experiment (NDCX).
**Issues to study:** fundamental limits of longitudinal compression, understand non-ideal experimental aspects, provide theory and simulation

**Primary component addition:**

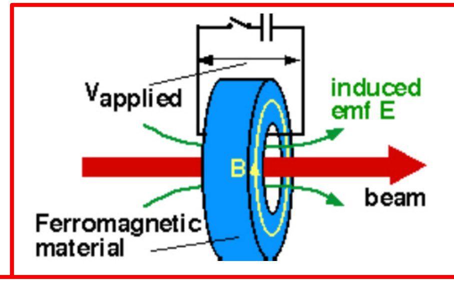


Single-gap linear induction accelerator induces pulsed **E**(t) along axis of beam to impose a head-to-tail axial *velocity tilt* on the passing ion beam

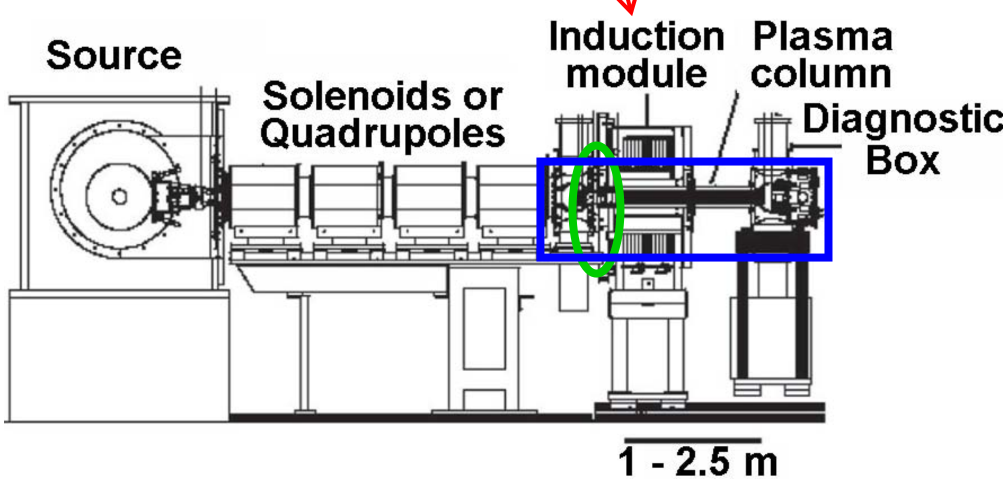


**Particle-in-cell simulations (LSP code):**
Used to model downstream end

The upgrade of NTX is the Neutralized Drift Compression Experiment (NDCX).
**Issues to study:** fundamental limits of longitudinal compression, understand non-ideal experimental aspects, provide theory and simulation

**Primary component addition:**

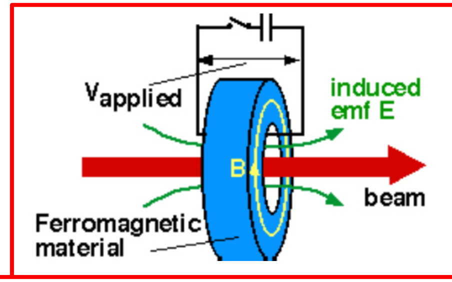


Single-gap linear induction accelerator induces pulsed **E**(t) along axis of beam to impose a head-to-tail axial *velocity tilt* on the passing ion beam

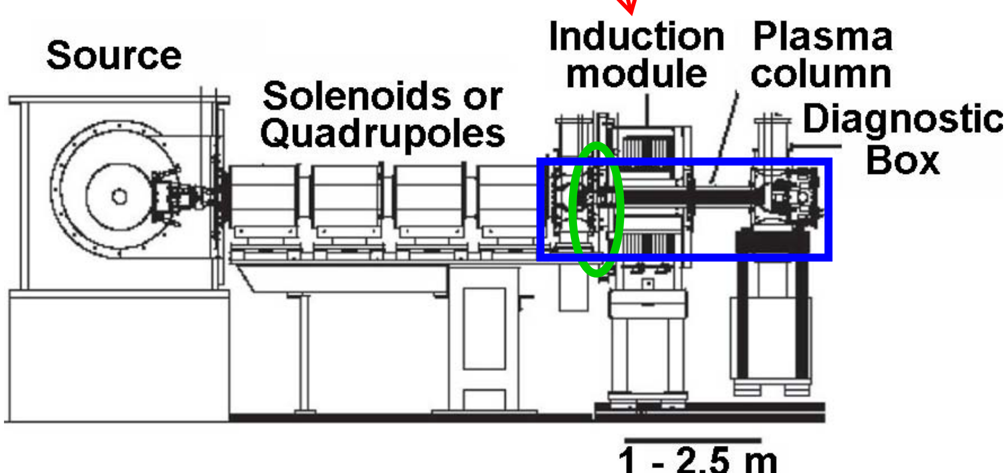


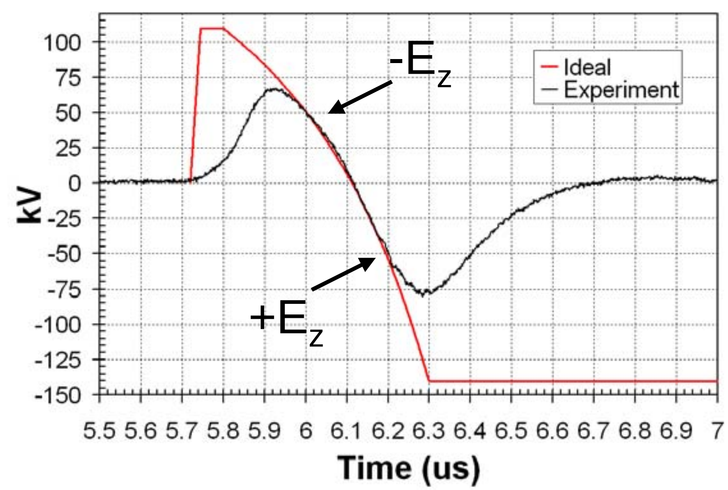


**Particle-in-cell simulations (LSP code):**
Used to model downstream end

**Figures of merit at the focal plane:**
Current compression ratio $I_b^{max}/I_0$
Full-width, half-maximum pulse length $t_{fwhm}$

# Outline

0) MOTIVATION AND ISSUES
- a) Overview
- b) Plasma neutralization-assisted focusing of space-charge-dominated beams

1) LONGITUDINAL COMPRESSION: ACCELERATION GAP EFFECTS
- a) Finite-size gap and voltage waveform
- b) Non-zero initial beam temperature (emittance)
- c) Initial pulse length $t_p$, intended fractional tilt *f*, and initial beam energy
- d) Comparison: theoretical models, particle-in-cell simulation, and experiment

2) TIME-DEPENDENT TRANSVERSE DEFOCUSING EFFECT OF THE ACCELERATION GAP
- a) Description of the effect
- b) The “over-focusing” technique for simultaneous transverse and longitudinal compression

3) SIMULTANEOUS FOCUSING USING A STRONG FINAL-FOCUS SOLENOID
- a) Focal plane aberration due to static magnetic field and beam velocity tilt
- b) Supersonic cathodic-arc plasma injection into the high-field region from the low-field end
- c) Collective excitations during the beam-plasma interaction for $n_b > n_p$

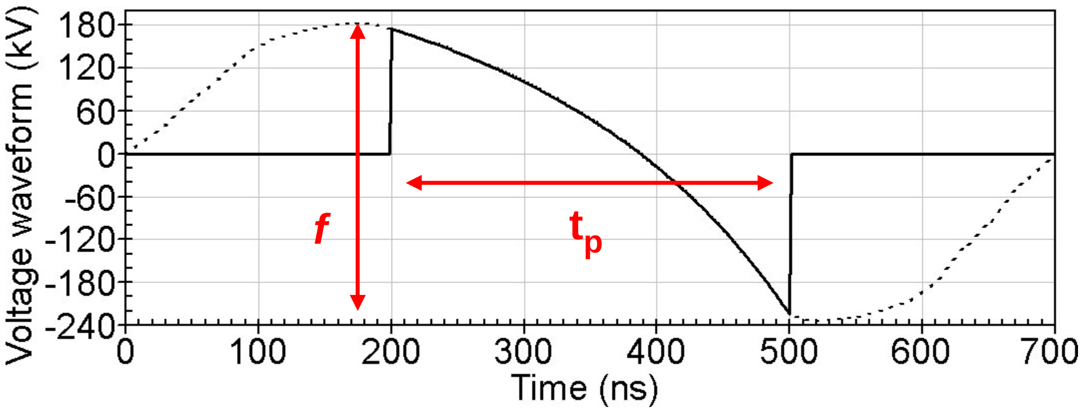


Generally, excess beam used ($t_p$ > 300 ns)

**Ideal waveform (dV/dt < 0) depends on:**

Initial beam energy: $E_0$ = 400 keV
Initial pulse length: $t_p$ = 300 ns
Intended fractional tilt: $f = 0.5 = \Delta v/v_0$

Resulting drift length: $L_d$ = 78.7 cm

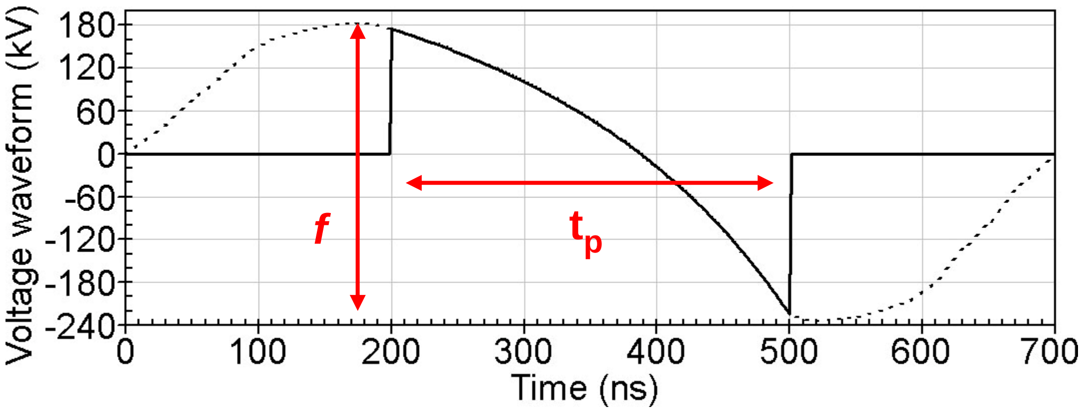


Generally, excess beam used ($t_p$ > 300 ns)

**Ideal waveform (dV/dt < 0) depends on:**

Initial beam energy: $E_0$ = 400 keV
Initial pulse length: $t_p$ = 300 ns
Intended fractional tilt: $f = 0.5 = \Delta v/v_0$

Resulting drift length: $L_d$ = 78.7 cm

The actual $\Delta z$ = 3 cm acceleration gap on NDCX

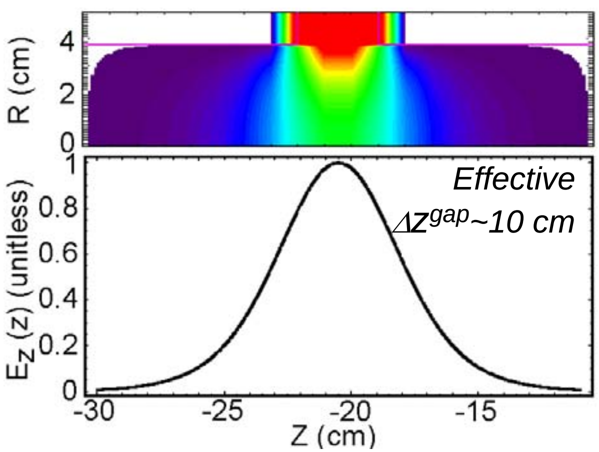


The transit time of a 400 keV $K^+$ particle across the "3 cm" gap is about 75 ns.

In this coordinate system:
z = {-30 cm, +100 to +250 cm}

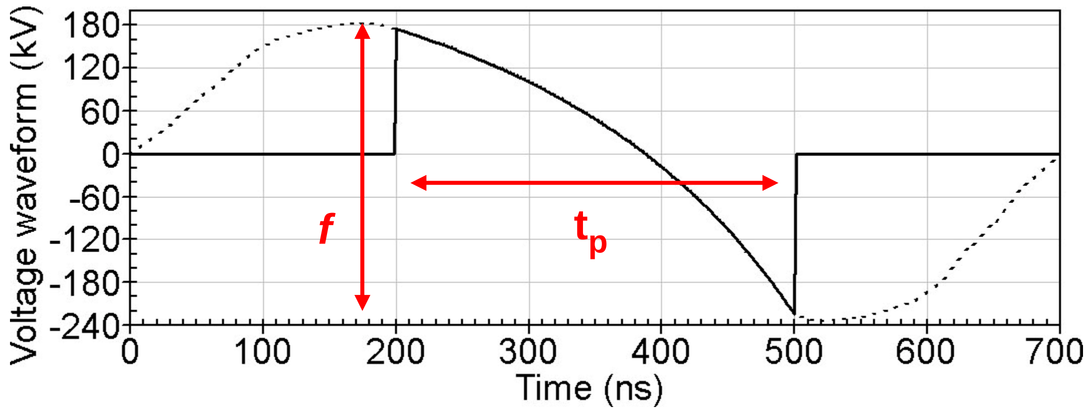


Generally, excess beam used ($t_p$ > 300 ns)

**Ideal waveform (dV/dt < 0) depends on:**

Initial beam energy: $E_0$ = 400 keV
Initial pulse length: $t_p$ = 300 ns
Intended fractional tilt: $f = 0.5 = \Delta v/v_0$

Resulting drift length: $L_d$ = 78.7 cm

Particles sample too much of the V(t) during their transit time across the gap. The integrated force over the gap is less than the intended amount to achieve the desired *f* = 0.5.

The actual $\Delta z$ = 3 cm acceleration gap on NDCX

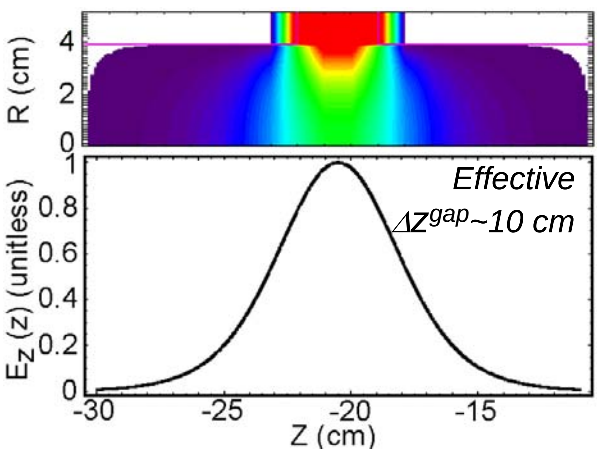


The transit time of a 400 keV $K^+$ particle across the "3 cm" gap is about 75 ns.

In this coordinate system:
z = {-30 cm, +100 to +250 cm}

The extra voltage in the "realistic" waveform across the finite-size gap re-populates some of the head and tail of the velocity tilt with the excess beam.

# Finite-size gap imparts velocity spread akin to temperature to beam

Electric field isocontours

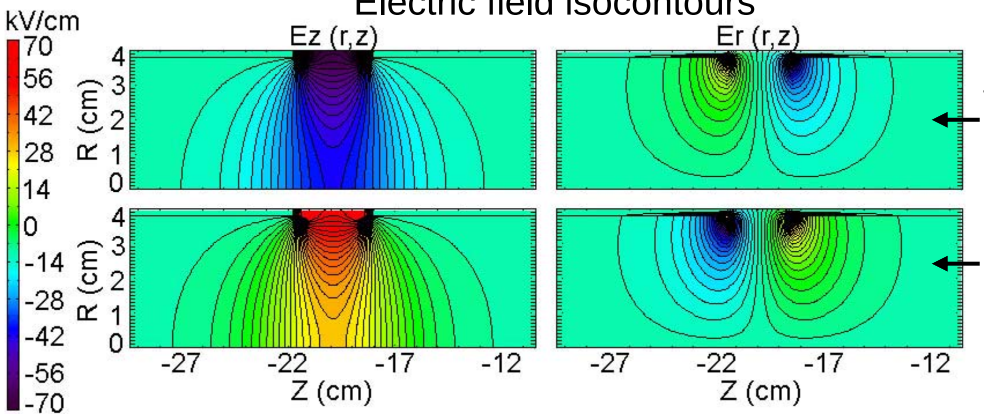


t = 200 ns
[max. V(t)]

t = 500 ns
[min. V(t)]

<u>Transverse and longitudinal phase space coupling effect within the gap:</u>
transit time and V(t) cause an +$\mathbf{E_r}$(r,z,t) imbalance, and radial movement within gap implies the dependence of integrated $\mathbf{E_z}$ on particle radius entering the gap

# Finite-size gap imparts velocity spread akin to temperature to beam

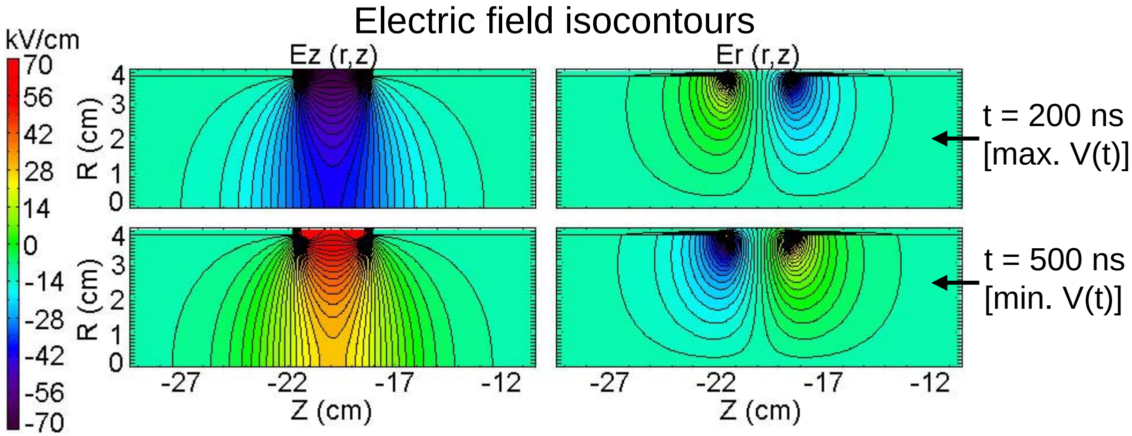


The initial $T_b$ = 0 eV beam gains effective longitudinal temperature from the gap, which sets a finite upper bound to the compression due to associated chromatic aberration.

<u>Transverse and longitudinal phase space coupling effect within the gap:</u> transit time and V(t) cause an +$\mathbf{E_r}$(r,z,t) imbalance, and radial movement within gap implies the dependence of integrated $\mathbf{E_z}$ on particle radius entering the gap

{z, $v_z$} beam phase space at the longitudinal focal plane

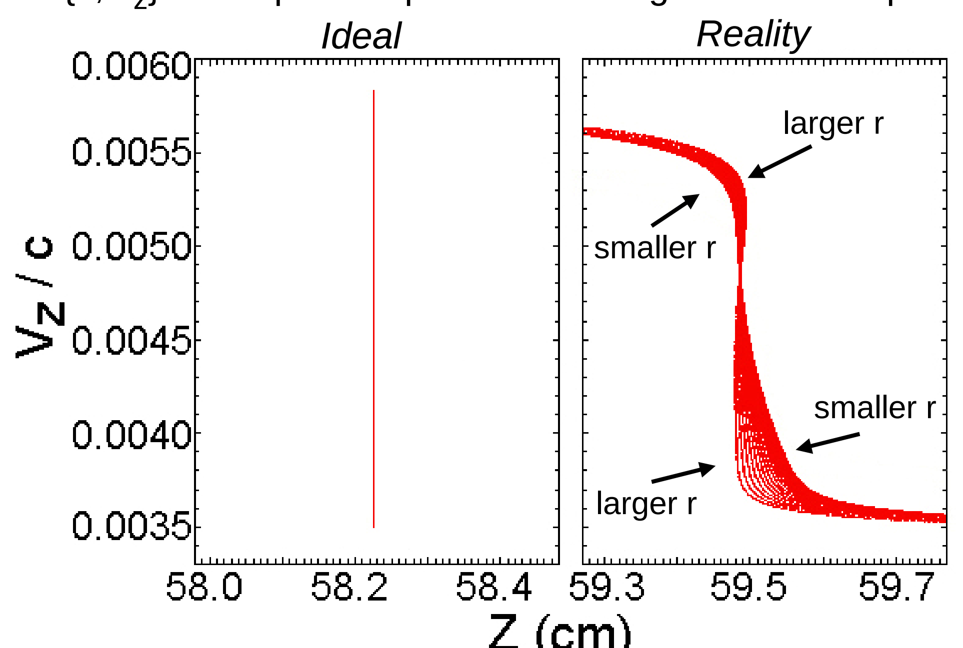

# Outline

0) MOTIVATION AND ISSUES

a) Overview

b) Plasma neutralization-assisted focusing of space-charge-dominated beams

1) LONGITUDINAL COMPRESSION: ACCELERATION GAP EFFECTS

a) Finite-size gap and voltage waveform

b) Non-zero initial beam temperature (emittance)

c) Initial pulse length $t_p$, intended fractional tilt *f*, and initial beam energy

d) Comparison: theoretical models, particle-in-cell simulation, and experiment

2) TIME-DEPENDENT TRANSVERSE DEFOCUSING EFFECT OF THE ACCELERATION GAP

a) Description of the effect

b) The “over-focusing” technique for simultaneous transverse and longitudinal compression

3) SIMULTANEOUS FOCUSING USING A STRONG FINAL-FOCUS SOLENOID

a) Focal plane aberration due to static magnetic field and beam velocity tilt

b) Supersonic cathodic-arc plasma injection into the high-field region from the low-field end

c) Collective excitations during the beam-plasma interaction for $n_b > n_p$

# Longitudinal compression demonstrates $\sqrt{T_b}$ dependence

Compression at focal plane for various initial $T_b$

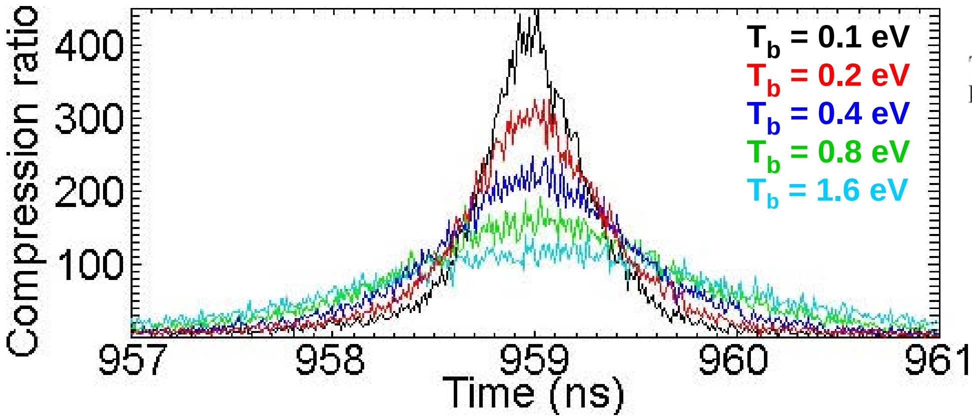


(*e.g.* $T_b$ = 0.2 eV → $\varepsilon_n^{4rms}$ = 9.3x10$^{-3}$ cm-mrad )

Table 4.1: Longitudinal compression dependence on initial emittance for $E_0$ = 400 keV, $t_p$ = 300 ns, and $f$ = 0.5. The $T_b$ = 0 eV case is included for reference.

| $T_b$ (PIC) | $I_b^{max}/I_0$ (PIC) | $t_{fwhm}$ (PIC) |
|---|---|---|
| 0 eV | 2650 | 0.035 ns |
| 0.1 eV | 430 | 0.51 ns |
| 0.2 eV | 320 | 0.70 ns |
| 0.4 eV | 230 | 1.01 ns |
| 0.8 eV | 160 | 1.40 ns |
| 1.6 eV | 115 | 2.05 ns |
| | $\sim T_b^{-0.48}$ | $\sim T_b^{+0.5}$ |

**Reminder:**
$E_0$ = 400 keV
$t_p$ = 300 ns
$f$ = 0.5
$L_d$ = 78.7 cm

Compression at focal plane for various initial $T_b$

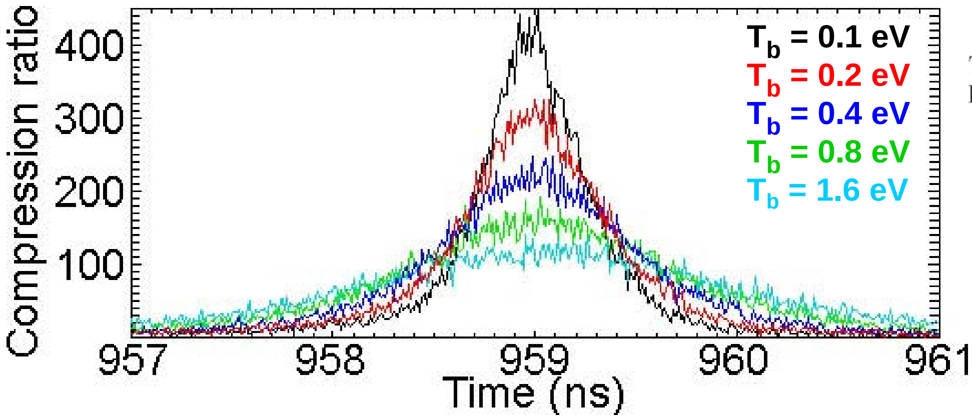


(*e.g.* $T_b$ = 0.2 eV → $\varepsilon_n^{4rms}$ = 9.3x10$^{-3}$ cm-mrad )

Table 4.1: Longitudinal compression dependence on initial emittance for $E_0 = 400$ keV, $t_p = 300$ ns, and $f = 0.5$. The $T_b = 0$ eV case is included for reference.

| $T_b$ (PIC) | $I_b^{max}/I_0$ (PIC) | $t_{fwhm}$ (PIC) |
|---|---|---|
| 0 eV | 2650 | 0.035 ns |
| 0.1 eV | 430 | 0.51 ns |
| 0.2 eV | 320 | 0.70 ns |
| 0.4 eV | 230 | 1.01 ns |
| 0.8 eV | 160 | 1.40 ns |
| 1.6 eV | 115 | 2.05 ns |
| | $\sim T_b^{-0.48}$ | $\sim T_b^{+0.5}$ |

**Reminder:**
$E_0$ = 400 keV
$t_p$ = 300 ns
$f$ = 0.5
$L_d$ = 78.7 cm

The gap and "realistic" waveform add an effective ~45% $T_{||}$ increase to the initial $T_b$ of the beam pulse, *for these parameters*, due to the reduction of the achieved *f** from the intended value *f*.

Comparison: infinitely thin gap and 3 cm gap

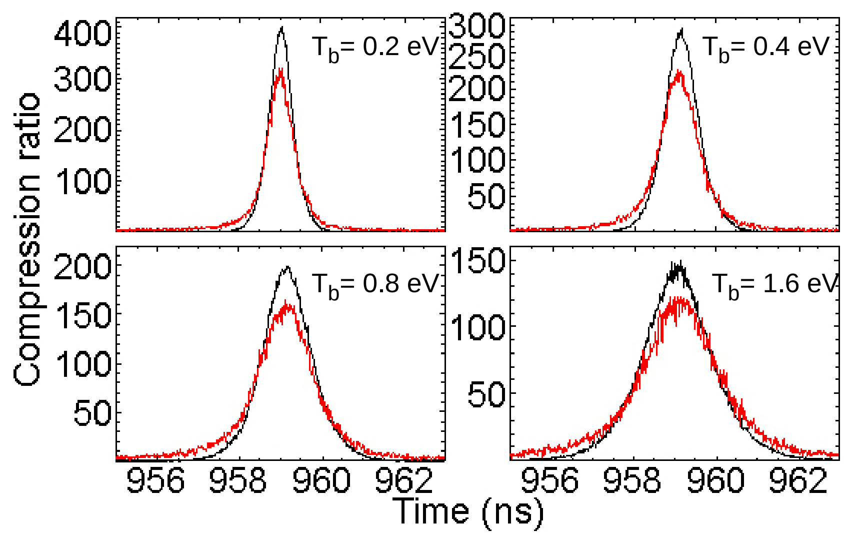


The geometrical constant [accounting for the acceleration gap and V(t) effects] depends on the gap geometry and V(t) compared to the pulse length and energy of the beam (as well as other beam parameters)

# Outline

0) MOTIVATION AND ISSUES

- a) Overview
- b) Plasma neutralization-assisted focusing of space-charge-dominated beams

1) LONGITUDINAL COMPRESSION: ACCELERATION GAP EFFECTS

- a) Finite-size gap and voltage waveform
- b) Non-zero initial beam temperature (emittance)
- c) Initial pulse length $t_p$, intended fractional tilt *f*, and initial beam energy
- d) Comparison: theoretical models, particle-in-cell simulation, and experiment

2) TIME-DEPENDENT TRANSVERSE DEFOCUSING EFFECT OF THE ACCELERATION GAP

- a) Description of the effect
- b) The "over-focusing" technique for simultaneous transverse and longitudinal compression

3) SIMULTANEOUS FOCUSING USING A STRONG FINAL-FOCUS SOLENOID

- a) Focal plane aberration due to static magnetic field and beam velocity tilt
- b) Supersonic cathodic-arc plasma injection into the high-field region from the low-field end
- c) Collective excitations during the beam-plasma interaction for $n_b > n_p$

# Voltage waveform parameter variation in $t_p$ with fixed $f$ and $E_0$

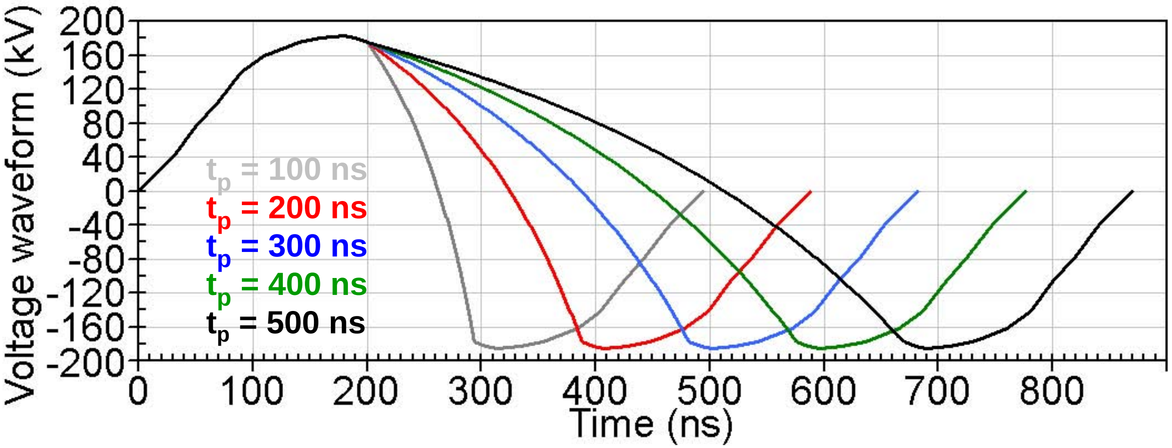

# Voltage waveform parameter variation in $t_p$ with fixed $f$ and $E_0$

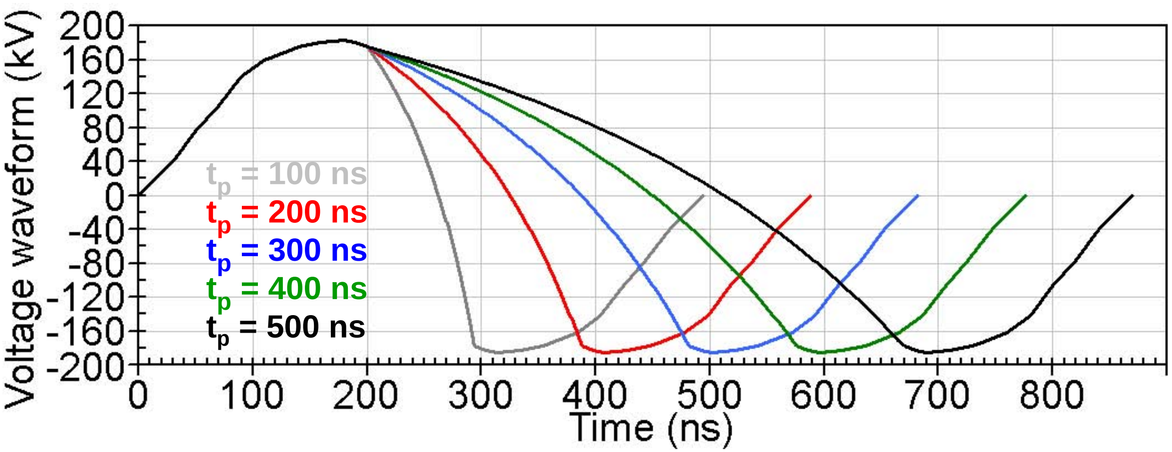


The compression ratios level off for larger $t_p$ with growing $t_{fwhm}$ due to increasing aberration from the longer drift lengths.

Table 4.2: Longitudinal compression dependence on initial pulse length $t_p$ for $E_0$ = 400 keV, $T_b$ = 0.2 eV, and an intended $f$ = 0.5.

| $t_p$ | $I_b^{max}/I_0$ | $t_{fwhm}$ | $L_d$ [Eq. (4.20)] | $t^{foc}$ (PIC) | $z^{foc}$ (PIC) |
|---|---|---|---|---|---|
| 100 ns | 120 | 0.5 ns | 26.2 cm | 468.3 ns | +8.4 cm |
| 200 ns | 220 | 0.6 ns | 52.5 cm | 710.5 ns | +33.5 cm |
| 300 ns | 280 | 0.7 ns | 78.7 cm | 959.0 ns | +59.5 cm |
| 400 ns | 310 | 0.9 ns | 104.9 cm | 1208.5 ns | +85.6 cm |
| 500 ns | 325 | 1.2 ns | 131.2 cm | 1457.5 ns | +111.7 cm |

leveling-off effect (~ $t_p^{0.3}$ for $t_p \geq 300$ ns)

grows ~linearly for $t_p \geq 300$ ns

Color-coded results (initial $T_b$ = 0.2 eV) at longitudinal focus

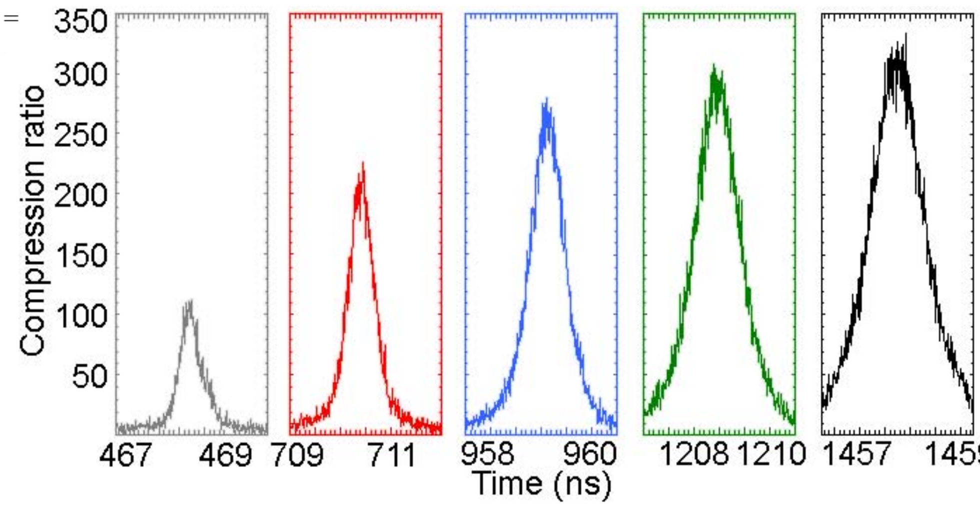

# Voltage waveform parameter variation in $f$ with fixed $t_p$ and $E_0$



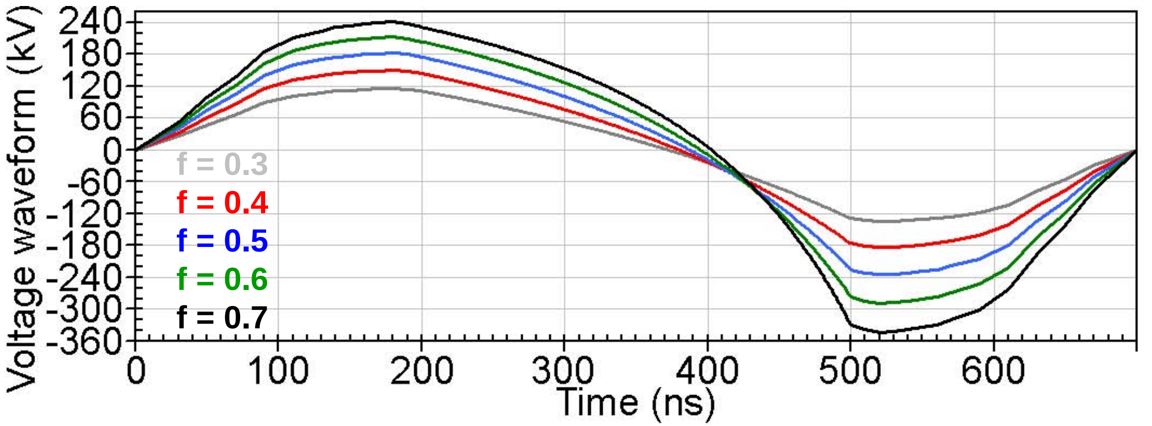


Larger tilts are generally desired for better compression, but are limited by the desired drift length to the focal plane, as well as voltage hold-off and transverse focusing aberration considerations

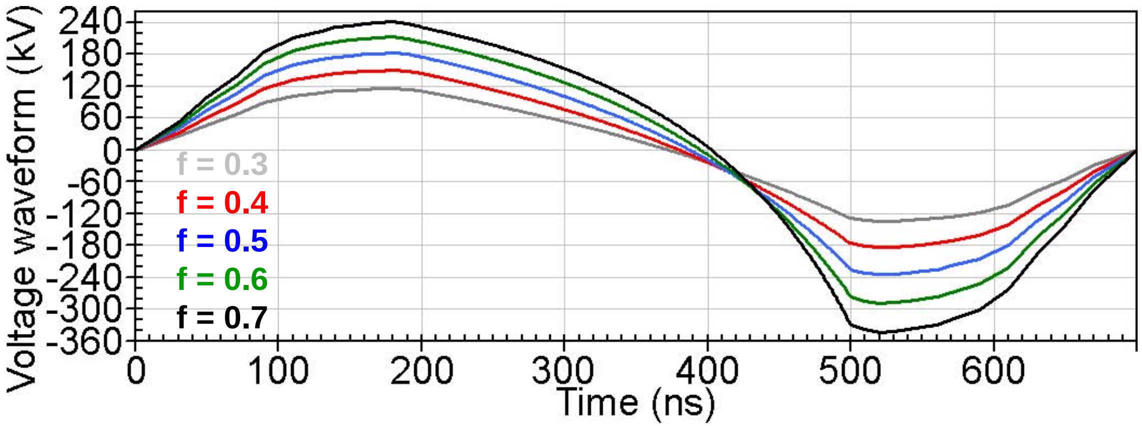


Larger tilts are generally desired for better compression, but are limited by the desired drift length to the focal plane, as well as voltage hold-off and transverse focusing aberration considerations

Table 4.3: Longitudinal compression dependence on intended fractional tilt $f$ for $E_0 = 400$ keV, $T_b = 0.2$ eV, and $t_p = 300$ ns.

| $f$ | $I_b^{max}/I_0$ | $t_{fwhm}$ | $L_d$ [Eq. (4.20)] | $t^{foc}$ (PIC) | $z^{foc}$ (PIC) |
|---|---|---|---|---|---|
| 0.3 | 210 | 1.4 ns | 136.8 cm | 1359.8 ns | +117.3 cm |
| 0.4 | 260 | 1.0 ns | 100.7 cm | 1109.0 ns | +81.5 cm |
| 0.5 | 320 | 0.7 ns | 78.7 cm | 959.0 ns | +59.5 cm |
| 0.6 | 360 | 0.6 ns | 63.7 cm | 859.1 ns | +44.5 cm |
| 0.7 | 380 | 0.5 ns | 52.6 cm | 787.8 ns | +33.5 cm |

~ $f^{0.82}$ for $f \leq 0.5$,

~ $f^{0.51}$ for $f \geq 0.5$

~ $f^{-1.23}$

Color-coded results (initial $T_b$ = 0.2 eV) at longitudinal focus

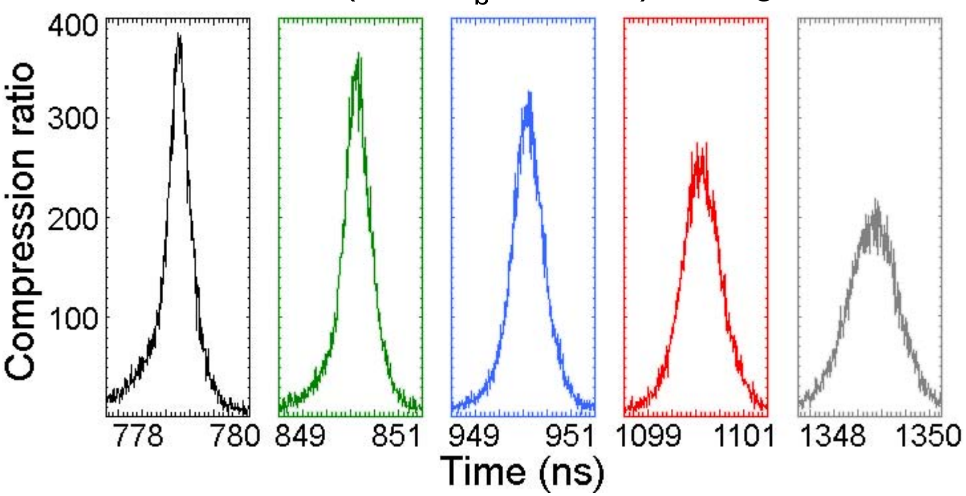

# Small (± 2.5 - 5%) constant $E_0$ shifts cause optimal focal plane degradation



Longitudinal compression at intended focal plane

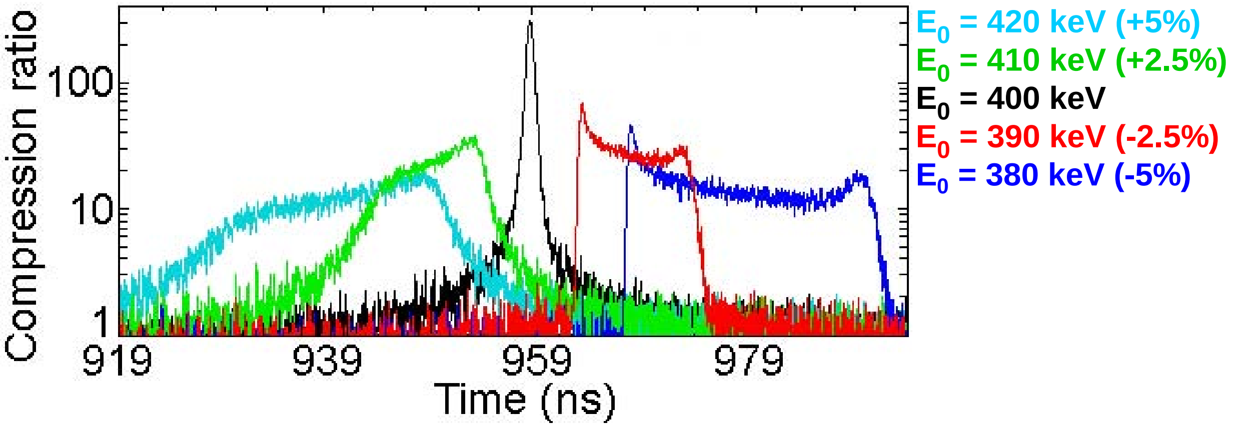


Beam energy accuracy in laboratory known to be approximately ≤ ±5%

# Small (± 2.5 - 5%) constant $E_0$ shifts cause optimal focal plane degradation

Longitudinal compression at intended focal plane

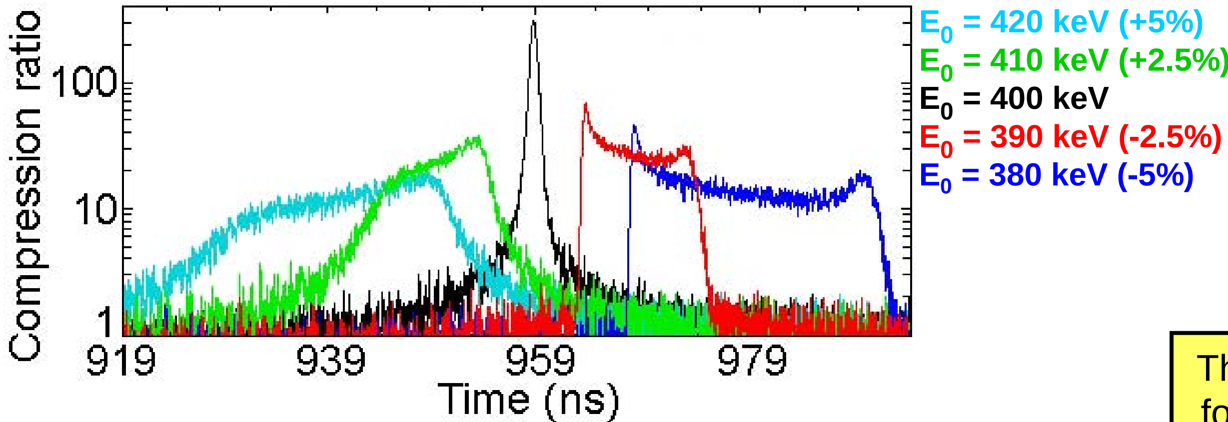


Beam energy accuracy in laboratory known to be approximately ≤ ±5%

The slope of the V(t) is only ideal for one particular $E_0$, and results in optimum compression only at one particular axial location.

Table 4.4: Longitudinal compression dependence on initial $E_b$ inaccuracy over a ±5% range with $T_b = 0.2$ eV for $E_0 = 400$ keV, $t_p = 300$ ns, and $f = 0.5$.

| $E_b$ | $I_b^{max}/I_0$ | $t_{fwhm}$ | $t^{foc}$ (PIC) | $z^{foc}$ (PIC) |
|---|---|---|---|---|
| 380 keV | 180 | 0.9 ns | 930.9 ns | +53.6 cm |
| 390 keV | 250 | 0.8 ns | 944.1 ns | +56.4 cm |
| 400 keV | 320 | 0.7 ns | 959.0 ns | +59.5 cm |
| 410 keV | 260 | 0.7 ns | 971.8 ns | +62.3 cm |
| 420 keV | 230 | 0.6 ns | 983.7 ns | +65.0 cm |

20-40% decrease from optimal

Color-coded results at the respective focal planes

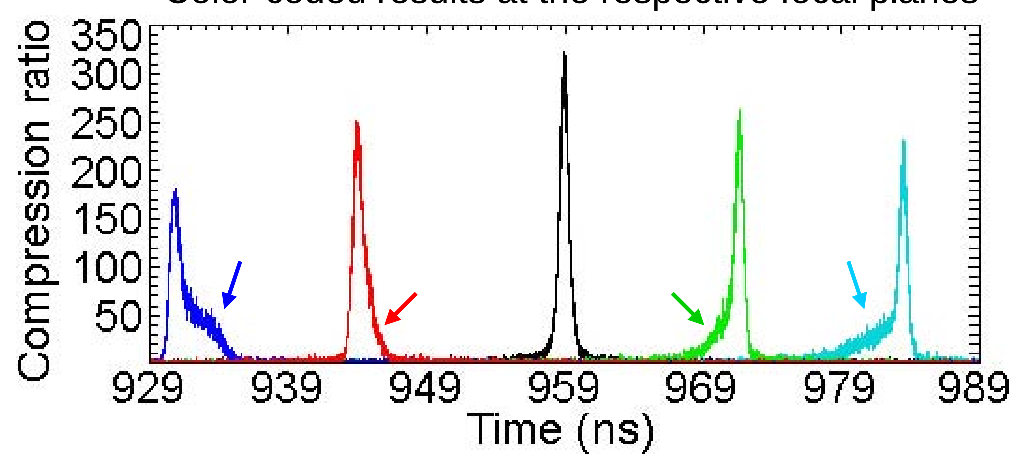


*Scan in $E_0$ with fixed V(t) and fixed diagnostic does not unambiguously determine optimum compression for a given V(t)*

# Small (± 2%) temporal $E_0(t)$ linear drifts cause optimal focal plane degradation

Longitudinal compression at respective focal planes

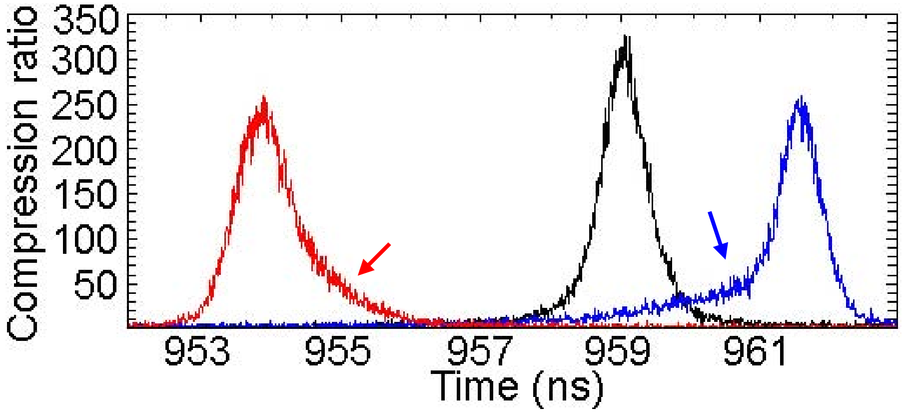


**$E_0$ = 400 keV**
**$E_0(t)$ = 400-408 keV (+2%)**
**$E_0(t)$ = 400-392 keV (-2%)**

$E_0$ may drift by ±1-2% over $t_p$ = 300 ns window in experiments

Table 4.5: Longitudinal compression dependence on initial linear increase or decrease in $E_b(t)$ by ±2% with $T_b = 0.2$ eV for $E_0 = 400$ keV, $t_p = 300$ ns, and $f = 0.5$.

| $E_b$ | $I_b^{max}/I_0$ | $t_{fwhm}$ | $t^{foc}$ (PIC) | $z^{foc}$ (PIC) |
|---|---|---|---|---|
| 400 – 392 keV | 250 | 0.8 ns | 961.5 ns | +59.3 cm |
| 400 keV | 320 | 0.7 ns | 959.0 ns | +59.5 cm |
| 400 – 408 keV | 250 | 0.8 ns | 953.9 ns | +59.3 cm |

22% decrease from optimal

Unintentional experimental beam energy inaccuracies, whether constant in time or not, will not reach the optimum compression compared to the desired $E_0$ for the specific V(t) under consideration.

# Outline

0) MOTIVATION AND ISSUES

a) Overview

b) Plasma neutralization-assisted focusing of space-charge-dominated beams

1) LONGITUDINAL COMPRESSION: ACCELERATION GAP EFFECTS

a) Finite-size gap and voltage waveform

b) Non-zero initial beam temperature (emittance)

c) Initial pulse length $t_p$, intended fractional tilt *f*, and initial beam energy

d) Comparison: theoretical models, particle-in-cell simulation, and experiment

2) TIME-DEPENDENT TRANSVERSE DEFOCUSING EFFECT OF THE ACCELERATION GAP

a) Description of the effect

b) The "over-focusing" technique for simultaneous transverse and longitudinal compression

3) SIMULTANEOUS FOCUSING USING A STRONG FINAL-FOCUS SOLENOID

a) Focal plane aberration due to static magnetic field and beam velocity tilt

b) Supersonic cathodic-arc plasma injection into the high-field region from the low-field end

c) Collective excitations during the beam-plasma interaction for $n_b > n_p$

# Excellent comparison to neutralized drift compression experiments

Initial $I_0$ ~ 20 mA, $r_b$ ~ 2 cm, $T_b$ ~ 0.2 eV

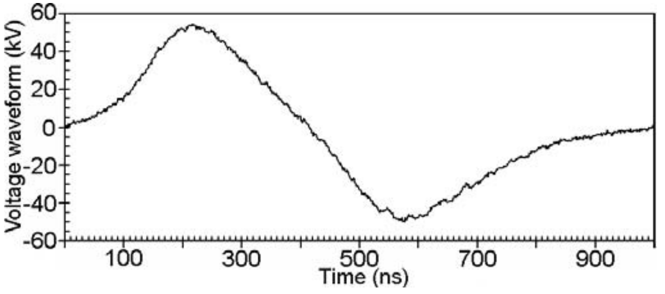


~2.4-m drift length for $E_0$ = 320 keV,
with $f^*_{exp}$ ~ 0.15

Initial $I_0$ ~ 20 mA, $r_b$ ~ 2 cm, $T_b$ ~ 0.2 eV

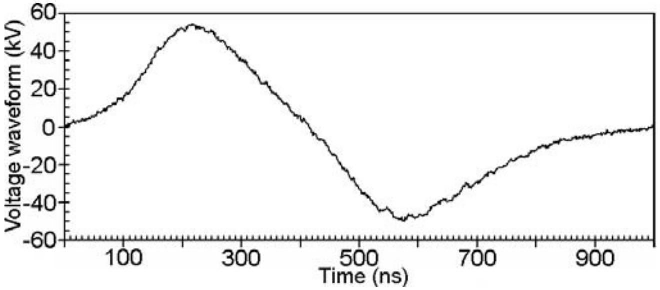


~2.4-m drift length for $E_0$ = 320 keV, with $f^*_{exp}$ ~ 0.15

Experiment and Simulation

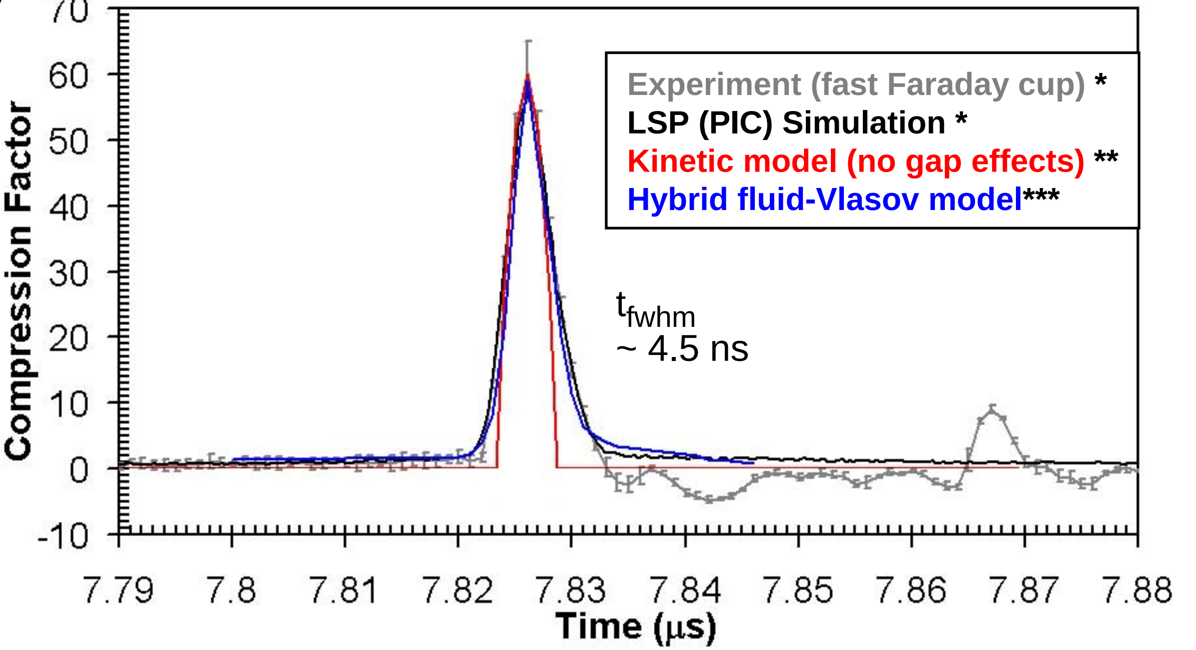


*A. B. Sefkow, et al., *Phys. Rev. ST Accel. Beams* **9**, 052801 (2006).
**R. C. Davidson and H. Qin, *Phys. Rev. ST Accel. Beams* **8**, 064201 (2005).
***A. B. Sefkow and R. C. Davidson, *Phys. Rev. ST Accel. Beams* **9**, 090101 (2006).

# Excellent comparison to neutralized drift compression experiments

Initial $I_0$ ~ 20 mA, $r_b$ ~ 2 cm, $T_b$ ~ 0.2 eV

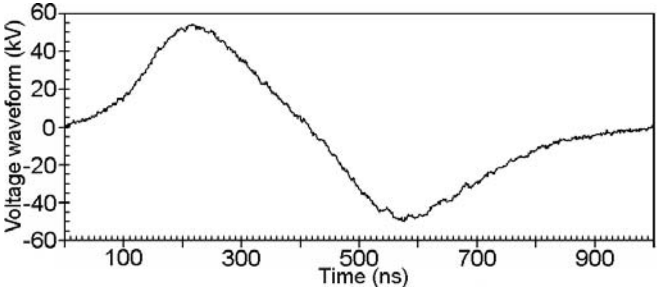


~2.4-m drift length for $E_0$ = 320 keV, with $f^*_{exp}$ ~ 0.15

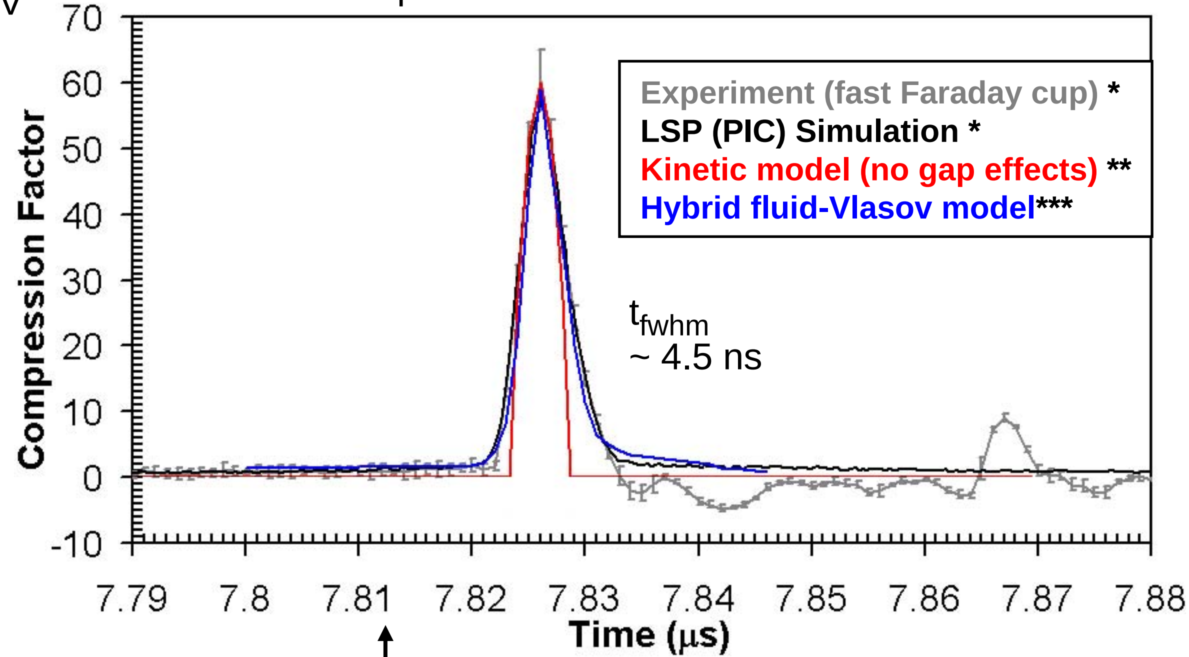


The new goal is to *simultaneously* focus such an axially compressed pulse **to a coincident focal plane** with a sub-mm radius for warm-dense-matter experiments.

However, $r_b^{foc}$ ~ 1 cm (reason explained next) → $J_z^{foc}/J_{z0}$ ~ 240 X

*A. B. Sefkow, et al., *Phys. Rev. ST Accel. Beams* **9**, 052801 (2006).
**R. C. Davidson and H. Qin, *Phys. Rev. ST Accel. Beams* **8**, 064201 (2005).
***A. B. Sefkow and R. C. Davidson, *Phys. Rev. ST Accel. Beams* **9**, 090101 (2006).

# Outline

0) MOTIVATION AND ISSUES

a) Overview

b) Plasma neutralization-assisted focusing of space-charge-dominated beams

1) LONGITUDINAL COMPRESSION: ACCELERATION GAP EFFECTS

a) Finite-size gap and voltage waveform

b) Non-zero initial beam temperature (emittance)

c) Initial pulse length $t_p$, intended fractional tilt *f*, and initial beam energy

d) Comparison: theoretical models, particle-in-cell simulation, and experiment

2) TIME-DEPENDENT TRANSVERSE DEFOCUSING EFFECT OF THE ACCELERATION GAP

a) Description of the effect

b) The "over-focusing" technique for simultaneous transverse and longitudinal compression

3) SIMULTANEOUS FOCUSING USING A STRONG FINAL-FOCUS SOLENOID

a) Focal plane aberration due to static magnetic field and beam velocity tilt

b) Supersonic cathodic-arc plasma injection into the high-field region from the low-field end

c) Collective excitations during the beam-plasma interaction for $n_b > n_p$

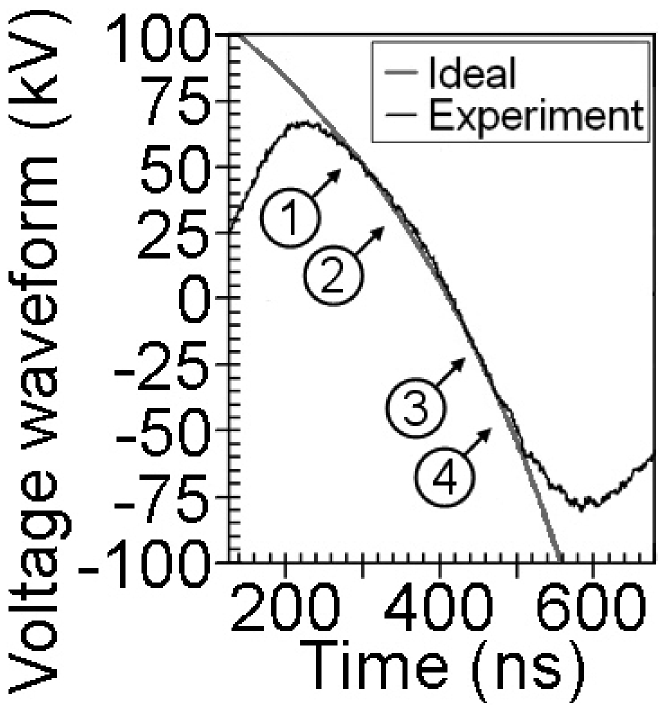


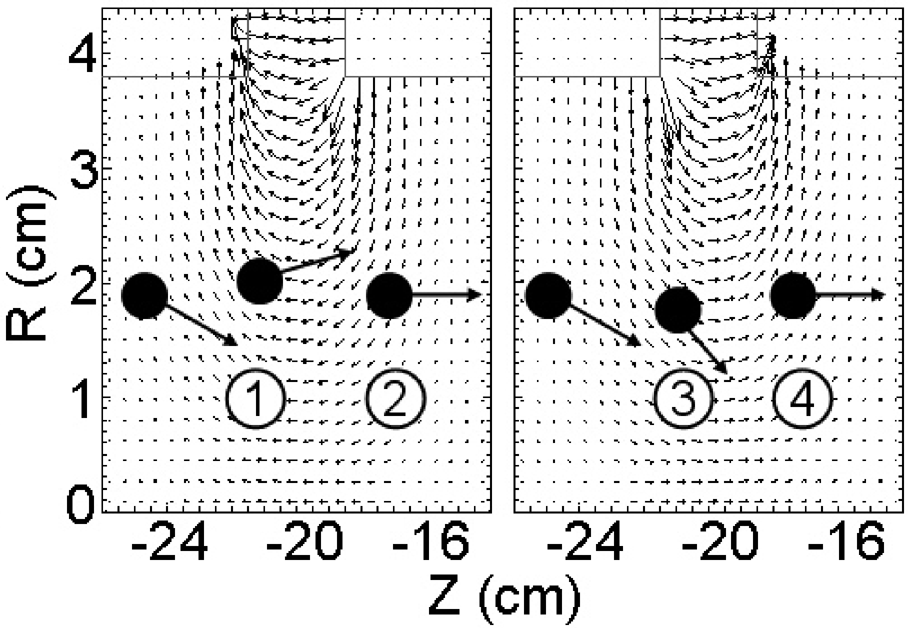


The defocusing effect occurs during the longitudinally compressing [dV(t)/dt < 0] portion of the waveform

*All particles participating in the axial velocity tilt receive a net divergence to their trajectories*

## Simulation

$\{z, r\}$ :

$\{z, v_r\}$ :

$\{z, v_z\}$ :

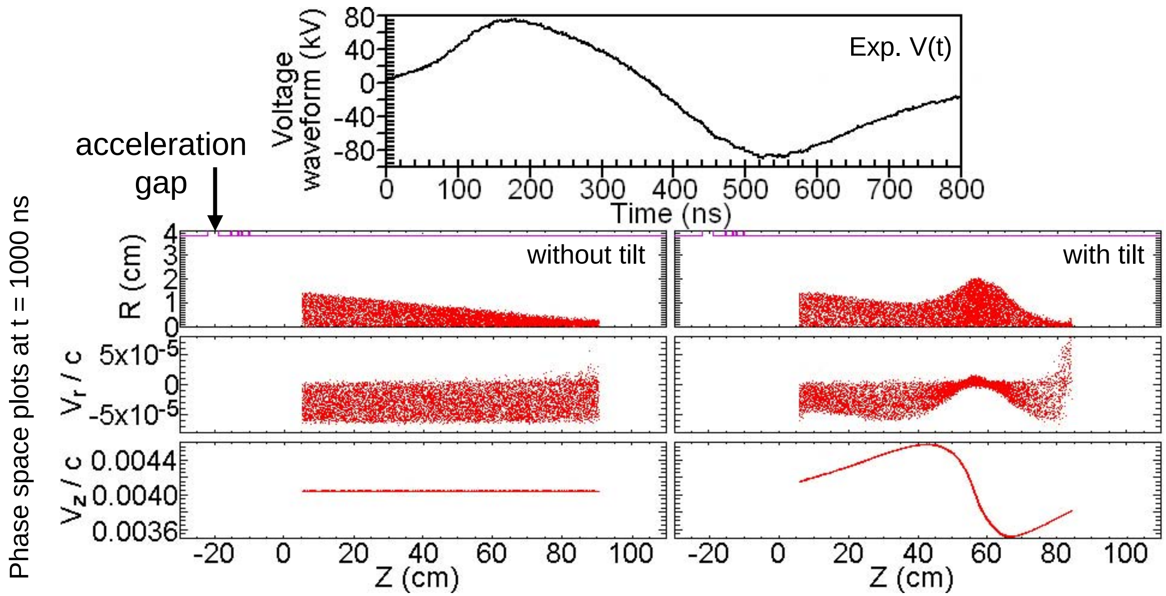


**Initial parameters:**
$E_0$ = 300 keV $K^+$
$r_b$ = 2 cm
$I_0$ = 18 mA
$T_b$ = 0.2 eV
$\Delta\theta_r$ = -15.4 mrad
$t_p$ = 700 ns

**Axial compression:**
$f^*_{exp} \sim 0.1$
$I_b^{max}/I_0 \sim 67$ X
$t_{fwhm} \sim 1.7$ ns
$r_b^{foc} \sim 2$ cm (flat-top)
$z^{foc}$ = +95 cm ($L_d \sim 1.15$ m)

## Simulation

{z, r} :

{z, $v_r$} :

{z, $v_z$} :

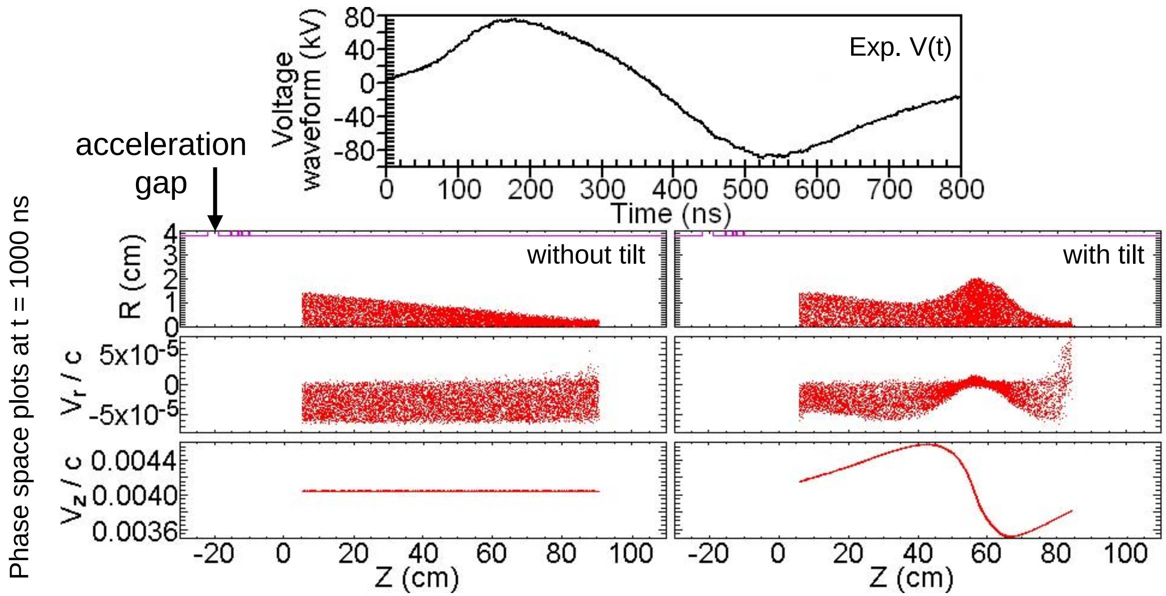


**Initial parameters:**
$E_0$ = 300 keV $K^+$
$r_b$ = 2 cm
$I_0$ = 18 mA
$T_b$ = 0.2 eV
$\Delta\theta_r$ = -15.4 mrad
$t_p$ = 700 ns

**Axial compression:**
$f^*_{exp}$ ~ 0.1
$I_b^{max}/I_0$ ~ 67 X
$t_{fwhm}$ ~ 1.7 ns
$r_b^{foc}$ ~ 2 cm (flat-top)
$z^{foc}$ = +95 cm ($L_d$ ~ 1.15 m)

Large spot sizes unusable for target heating experiments since $J_z \sim r_b(t)^{-2}$

## Experiment

P. K. Roy, et. al., *Phys. Rev. Lett.* 95, 234801 (2005)

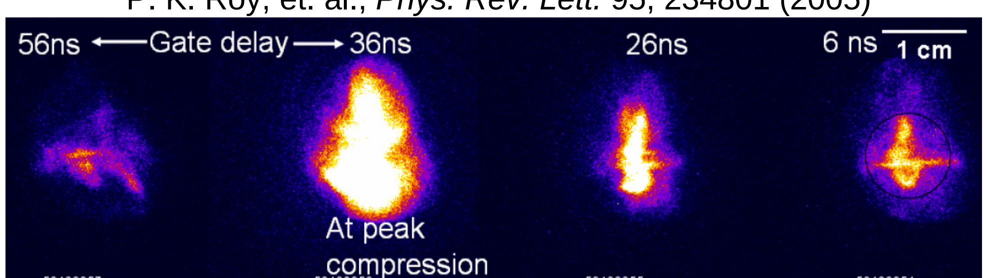

# Outline

0) MOTIVATION AND ISSUES
- a) Overview
- b) Plasma neutralization-assisted focusing of space-charge-dominated beams

1) LONGITUDINAL COMPRESSION: ACCELERATION GAP EFFECTS
- a) Finite-size gap and voltage waveform
- b) Non-zero initial beam temperature (emittance)
- c) Initial pulse length $t_p$, intended fractional tilt *f*, and initial beam energy
- d) Comparison: theoretical models, particle-in-cell simulation, and experiment

2) TIME-DEPENDENT TRANSVERSE DEFOCUSING EFFECT OF THE ACCELERATION GAP
- a) Description of the effect
- b) The "over-focusing" technique for simultaneous transverse and longitudinal compression

3) SIMULTANEOUS FOCUSING USING A STRONG FINAL-FOCUS SOLENOID
- a) Focal plane aberration due to static magnetic field and beam velocity tilt
- b) Supersonic cathodic-arc plasma injection into the high-field region from the low-field end
- c) Collective excitations during the beam-plasma interaction for $n_b > n_p$

## Simulation

Beam density isocontours

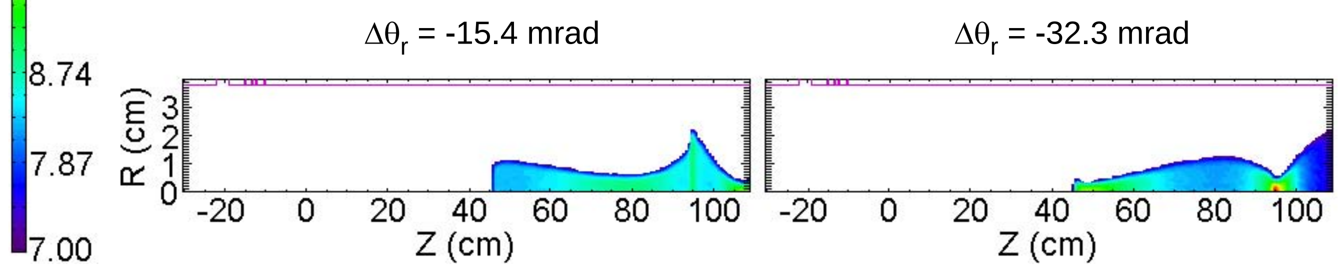


**Regular focus case:**
$n_b^{foc} \sim 1.4 \times 10^9$ cm$^{-3}$, $r_b^{foc} \sim 2$ cm

**Over-focused case:**
$n_b^{foc} \sim 2.3 \times 10^{11}$ cm$^{-3}$, $r_b^{foc} \sim 0.125$ cm

Over-focusing required to recover sufficient main pulse contrast and achieve desired $r_b^{foc}(t)$

## Simulation

Beam density isocontours

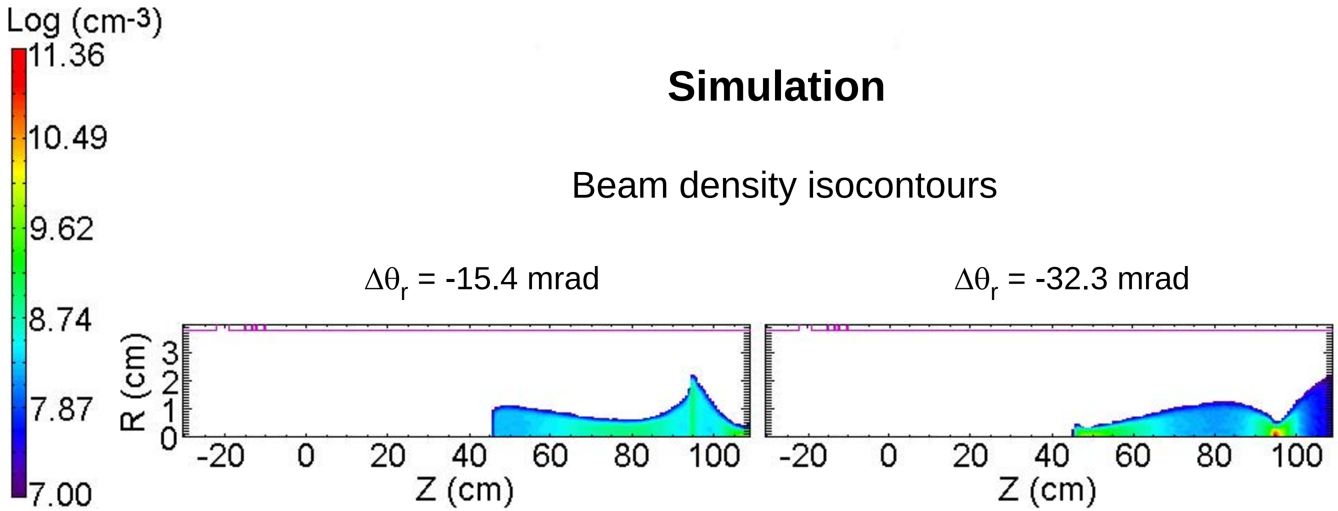


**Regular focus case:**
$n_b^{foc} \sim 1.4 \times 10^9$ cm$^{-3}$, $r_b^{foc} \sim 2$ cm

**Over-focused case:**
$n_b^{foc} \sim 2.3 \times 10^{11}$ cm$^{-3}$, $r_b^{foc} \sim 0.125$ cm

Over-focusing required to recover sufficient main pulse contrast and achieve desired $r_b^{foc}(t)$

## Experiment

**Poster tomorrow: J. E. Coleman [ THPAS004 ]**

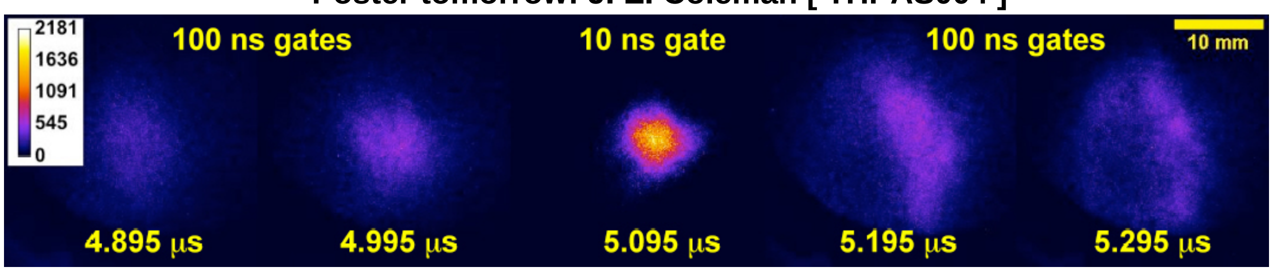


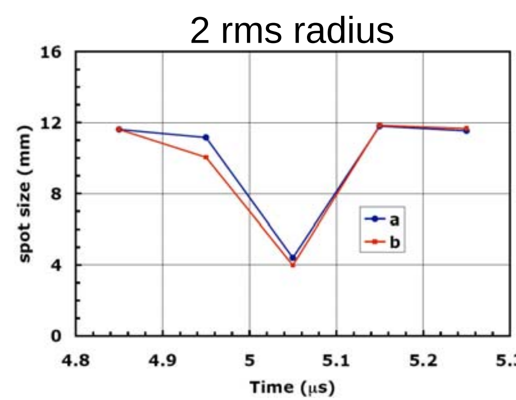

# Outline

0) MOTIVATION AND ISSUES
- a) Overview
- b) Plasma neutralization-assisted focusing of space-charge-dominated beams

1) LONGITUDINAL COMPRESSION: ACCELERATION GAP EFFECTS
- a) Finite-size gap and voltage waveform
- b) Non-zero initial beam temperature (emittance)
- c) Initial pulse length $t_p$, intended fractional tilt *f*, and initial beam energy
- d) Comparison: theoretical models, particle-in-cell simulation, and experiment

2) TIME-DEPENDENT TRANSVERSE DEFOCUSING EFFECT OF THE ACCELERATION GAP
- a) Description of the effect
- b) The “over-focusing” technique for simultaneous transverse and longitudinal compression

3) SIMULTANEOUS FOCUSING USING A STRONG FINAL-FOCUS SOLENOID
- a) Focal plane aberration due to static magnetic field and beam velocity tilt
- b) Supersonic cathodic-arc plasma injection into the high-field region from the low-field end
- c) Collective excitations during the beam-plasma interaction for $n_b > n_p$

# A strong final-focus solenoid can achieve better simultaneous focusing

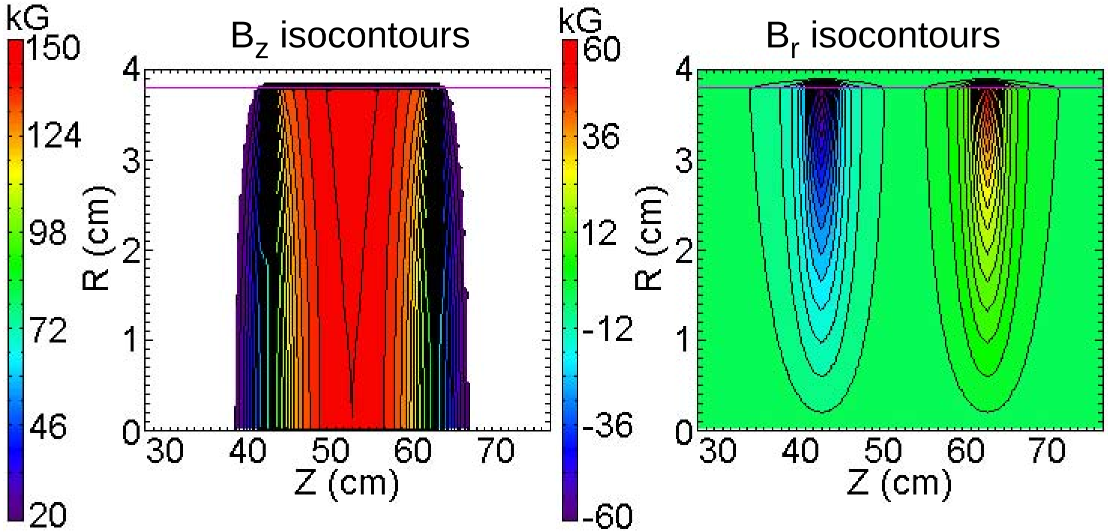


A final-focus solenoid transversely *re-focuses* the longitudinally compressing beam, *controls* the transverse focal length, and *reduces* the amount of $n_p$ needed upstream.

Here, $B_z$ = 150 kG (~140 kG at focus), $l^{sol}$ = 20 cm, $r^{sol}$ = 3.8 cm

*Amount of transverse compression sensitively depends on strength and positioning of solenoid*

# A strong final-focus solenoid can achieve better simultaneous focusing



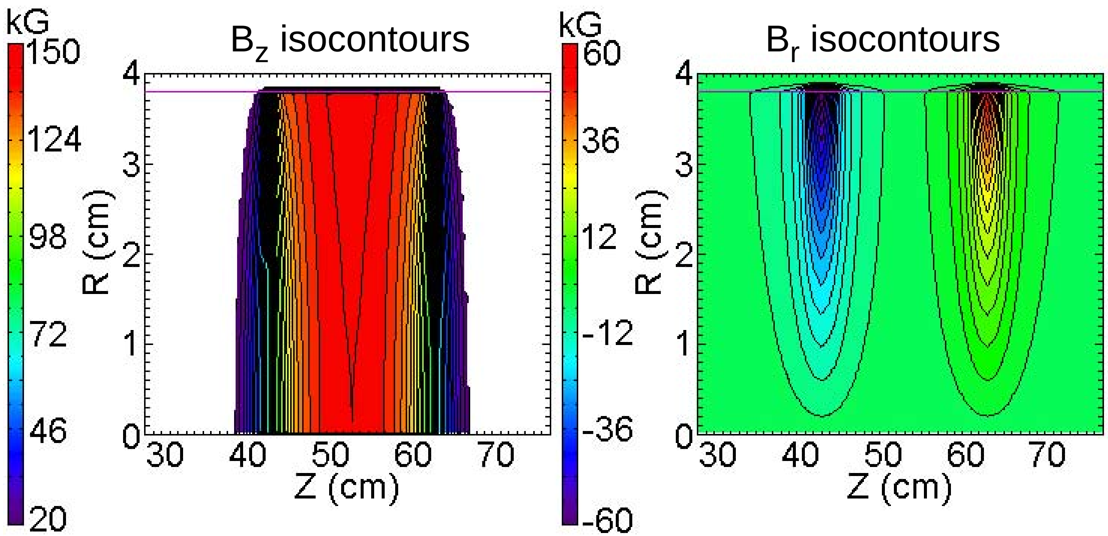


A final-focus solenoid transversely *re-focuses* the longitudinally compressing beam, *controls* the transverse focal length, and *reduces* the amount of $n_p$ needed upstream.

Here, $B_z$ = 150 kG (~140 kG at focus), $l^{sol}$ = 20 cm, $r^{sol}$ = 3.8 cm

*Amount of transverse compression sensitively depends on strength and positioning of solenoid*

**An axial velocity tilt contributes to focusing aberration within a final-focus solenoid**

Lower-energy head nominally focuses earlier in space and time
Higher-energy tail nominally focuses later in space and time

$-F_\theta = +q\,[(+v_z) \times (-B_r[r,z])] = -m_i\,(d\mathbf{v}/dt)_\theta$

$-F_r = +q\,[(-v_\theta) \times (+B_z[r,z])] = -m_i\,(d\mathbf{v}/dt)_r$

$\longrightarrow$

**Aberration depends on radius:**
beam particles entering the solenoid with same *z* (and E) but larger *r* acquire more $-v_\theta$ and will not focus at same location

*Ideal longitudinal compression across an infinitely thin gap*

Consider three cases of $J_z(t)$ and $r_b(t)$ entering the chosen static final-focus solenoid

*$r_b$ = 2 cm cases*

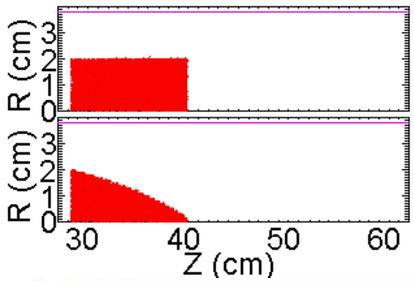


**1.** $r_b$ and $J_z$ constant (for $r_b$ = 1 & 2 cm)

**2.** $r_b(t)$ linear increase from $r_b$ = 0.1 to 1 & 2 cm over $t_p$, with $J_z(t) \sim r_b(t)^{-2}$ to maintain $I_0$ = 80 mA constant

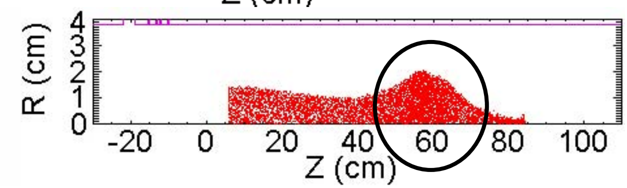


**3.** $r_b(t)$ linear increase from $r_b$ = 0.1 to 1 & 2 cm over 1st $t_p/2$ and linear decrease from $r_b$ = 1 & 2 to 0.1 cm over 2nd $t_p/2$, with $J_z(t) \sim r_b(t)^{-2}$ to maintain $I_0$ = 80 mA constant

**Case #3: The most "realistic" scenario, due to transverse defocusing effect**

**Beam parameters:**
$E_0$ = 400 keV
$t_p$ = 300 ns
$f$ = 0.5
$L_d$ = 78.7 cm

$I_0$ = 80 mA
$T_b$ = 0.2 eV
$\Delta\theta_r$ = 0 mrad

Intended:
$I_b^{max}/I_0$ = 400
$t_{fhwm}$ = 0.6 ns
$z^{foc}$ = +58.25 cm

*Ideal longitudinal compression across an infinitely thin gap*

Consider three cases of $J_z(t)$ and $r_b(t)$ entering the chosen static final-focus solenoid

*$r_b$ = 2 cm cases*

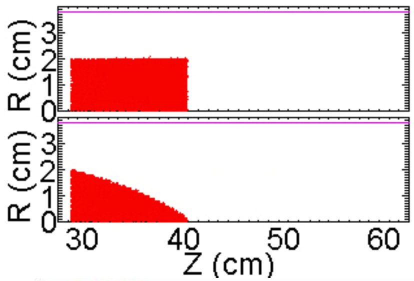


**1.** $r_b$ and $J_z$ constant (for $r_b$ = 1 & 2 cm)

**2.** $r_b(t)$ linear increase from $r_b$ = 0.1 to 1 & 2 cm over $t_p$, with $J_z(t) \sim r_b(t)^{-2}$ to maintain $I_0$ = 80 mA constant

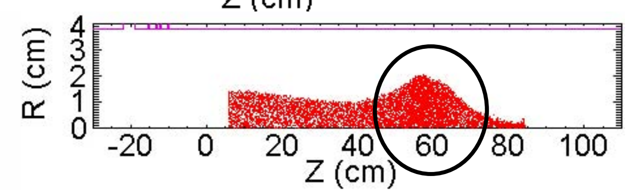


**3.** $r_b(t)$ linear increase from $r_b$ = 0.1 to 1 & 2 cm over 1st $t_p/2$ and linear decrease from $r_b$ = 1 & 2 to 0.1 cm over 2nd $t_p/2$, with $J_z(t) \sim r_b(t)^{-2}$ to maintain $I_0$ = 80 mA constant

**Case #3: The most "realistic" scenario, due to transverse defocusing effect**

**Beam parameters:**
$E_0$ = 400 keV
$t_p$ = 300 ns
$f$ = 0.5
$L_d$ = 78.7 cm

$I_0$ = 80 mA
$T_b$ = 0.2 eV
$\Delta\theta_r$ = 0 mrad

Intended:
$I_b^{max}/I_0$ = 400
$t_{fhwm}$ = 0.6 ns
$z^{foc}$ = +58.25 cm

Can reduce aberration by allowing faster particles (arriving later) to have larger $r_b$ entering the solenoid

Slower head particles: desire weaker $-B_r$ to focus later t / longer z
Faster tail particles: desire stronger $-B_r$ to focus earlier t / shorter z

**yes**

**Rationale for Case #2: (expecting it to minimize aberration)** → $-B_r(r) \sim r^1$ for most $r < r^{sol}$ and $v_z$ tilt approx. linear

# Focusing improved by factors of 2 to 5 compared to constant $r_b$ cases

Cumulative energy deposition profiles

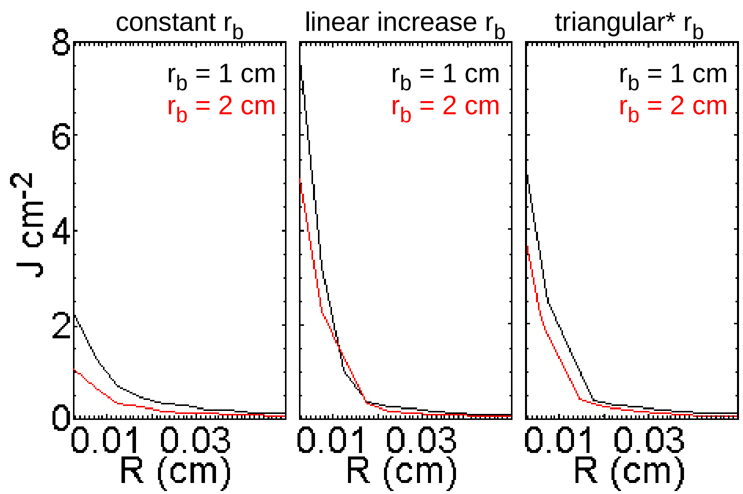


The defocusing effect provides a *beneficial** $r_b(t)$ for simultaneous focusing using final-focus solenoids relative to constant $r_b$ cases

Table 6.2: Compression dependence on initial $r_b(t)$ profile using a 150 kG solenoid.

| | Initial $r_b(t)$ | $I_b^{max}/I_0$ | $t_{fwhm}$ | $E_{dep}^{peak}$ | $r_b^{foc}$ $(1/e)$ |
|---|---|---|---|---|---|
| | 2 cm, constant | 100 | 2.7 ns | 1.1 J cm$^{-2}$ | 0.011 cm |
| | 1 cm, constant | 310 | 0.8 ns | 2.3 J cm$^{-2}$ | 0.011 cm |
| * | 2 cm, triangular | 275 | 0.8 ns | 3.8 J cm$^{-2}$ | 0.010 cm |
| * | 1 cm, triangular | 375 | 0.7 ns | 5.3 J cm$^{-2}$ | 0.010 cm |
| | 2 cm, linear increase | 290 | 1.0 ns | 5.0 J cm$^{-2}$ | 0.010 cm |
| | 1 cm, linear increase | 400 | 0.6 ns | 7.7 J cm$^{-2}$ | 0.008 cm |

Longitudinal — Transverse

← Nominal longitudinal compression recovered.
~ 8 GW cm$^{-2}$ on-axis peak, and total $J_z$ compression > $10^6$

# Outline

0) MOTIVATION AND ISSUES
- a) Overview
- b) Plasma neutralization-assisted focusing of space-charge-dominated beams

1) LONGITUDINAL COMPRESSION: ACCELERATION GAP EFFECTS
- a) Finite-size gap and voltage waveform
- b) Non-zero initial beam temperature (emittance)
- c) Initial pulse length $t_p$, intended fractional tilt *f*, and initial beam energy
- d) Comparison: theoretical models, particle-in-cell simulation, and experiment

2) TIME-DEPENDENT TRANSVERSE DEFOCUSING EFFECT OF THE ACCELERATION GAP
- a) Description of the effect
- b) The “over-focusing” technique for simultaneous transverse and longitudinal compression

3) SIMULTANEOUS FOCUSING USING A STRONG FINAL-FOCUS SOLENOID
- a) Focal plane aberration due to static magnetic field and beam velocity tilt
- b) Supersonic cathodic-arc plasma injection into the high-field region from the low-field end
- c) Collective excitations during the beam-plasma interaction for $n_b > n_p$

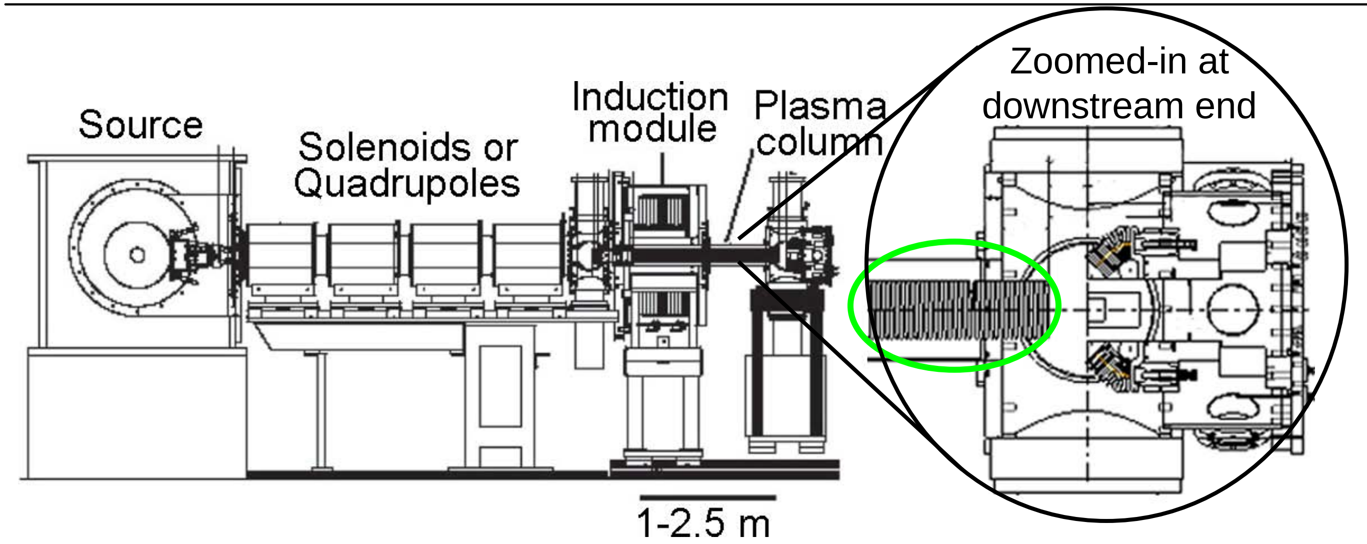


Can supersonic cathodic-arc $Al^+$ plasma be injected into the **high-field** region?

**Variable solenoid strength:**
$B_y$ ~ 2 kG (guide field for creating plasma column)

*or*

$B_y$ ~ 30-150 kG for transverse final-focus

**Does the magnetic mirroring effect prevent the plasma flow?**

# 3D filtered cathodic-arc plasma source geometry and magnetic field topology

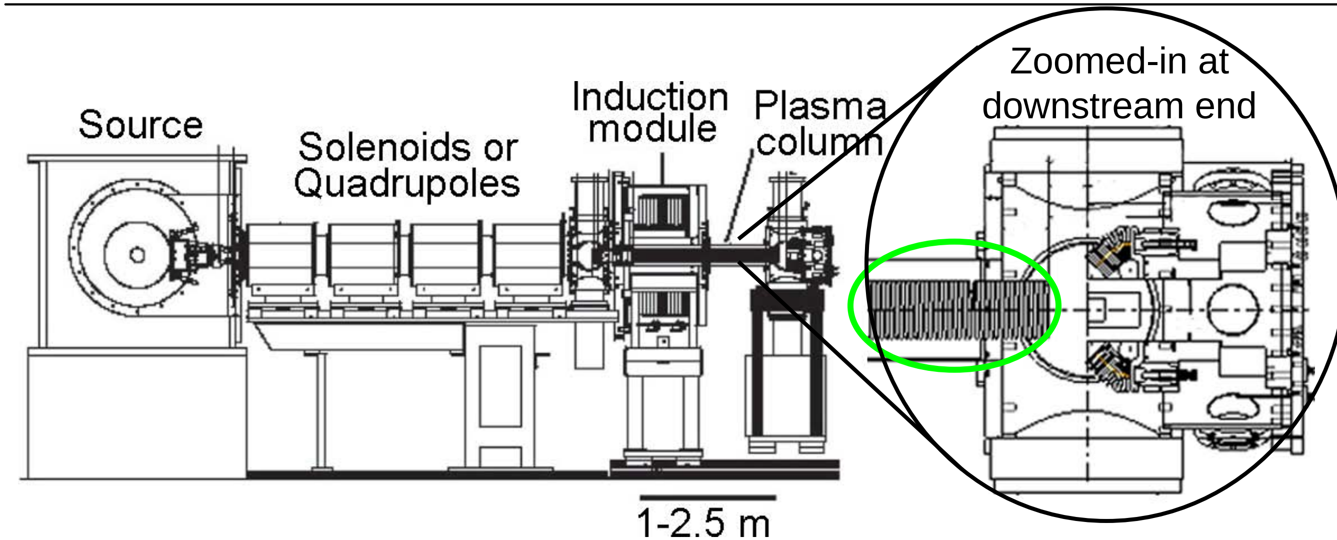


Can supersonic cathodic-arc *Al*$^+$ plasma be injected into the **high-field** region?

Coordinate switch: +z direction now -y direction

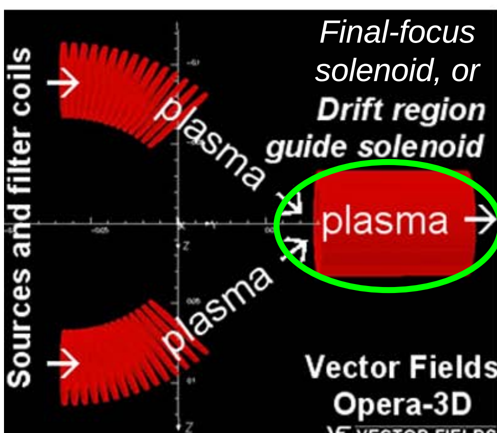


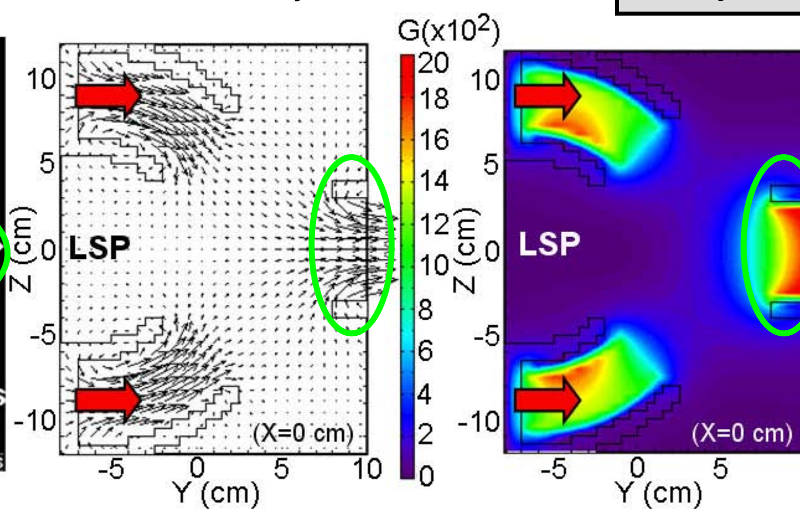


**Variable solenoid strength:**
$B_y$ ~ 2 kG (guide field for creating plasma column)

*or*

$B_y$ ~ 30-150 kG for transverse final-focus

**Does the magnetic mirroring effect prevent the plasma flow?**

Injection into **53 kG** final-focus solenoid with filter coils operating at 0.45 kG.

$v_y^i$ ~ 1.44 cm/μs
(~29 eV, measured)

$T_i$ ~ 3 eV and $T_e$ ~ 10 eV
is an ion mach speed $M_i$ ~ 1.7

$J_{p0}$ ~ 2 A $cm^{-2}$ in each
filter coil (~$10^{13}$ $cm^{-3}$ peak)

Plasma density {y,z} isocontours through x = 0 slices

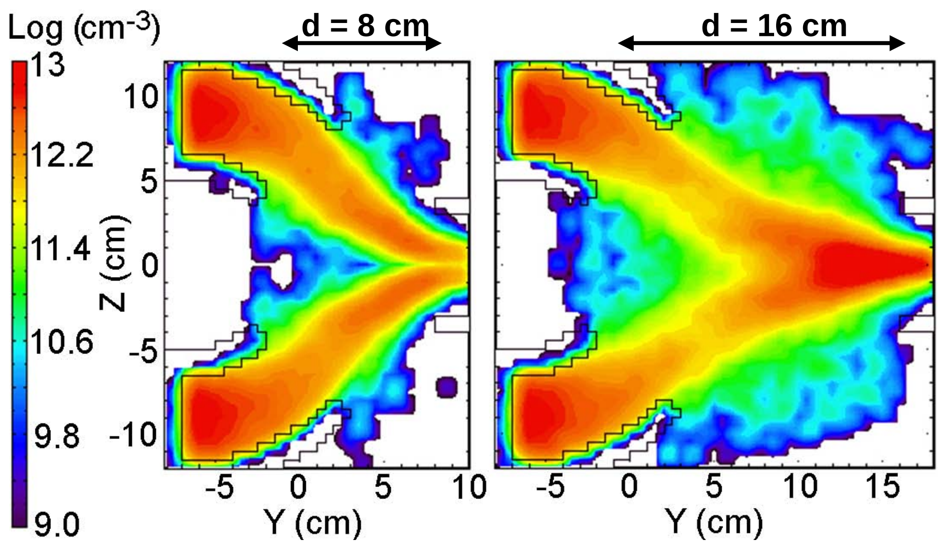

Plasma injection occurs at z~18 cm in upstream (-z) direction

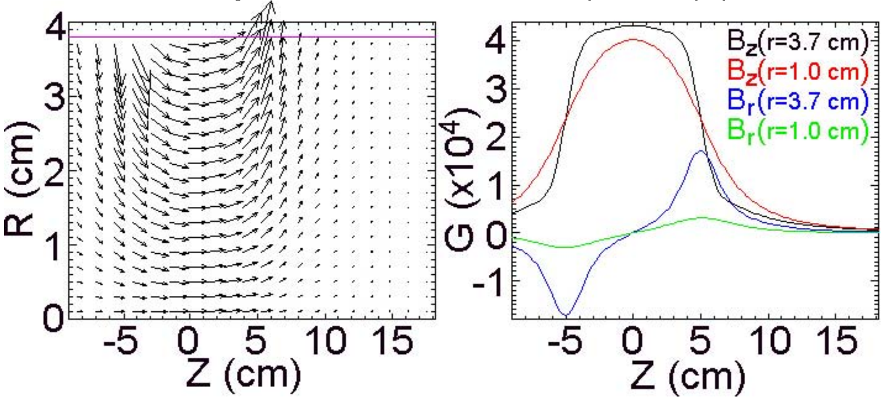


Assumption (from reduced dimensionality): $J_z^i$ ~ 0.3, 0.6, 1.2, 2.4 A $cm^{-2}$ with constant $n_p$ ~ $10^{12}$ $cm^{-3}$ at injection plane

**4 cases:**

$v_z^i$ = -1.5, -3, -6, -12 cm/$\mu$s
$T_i$ ~ 1 eV and $T_e$ ~ 5 eV
($M_i$ ~ 2.7, 5.5, 11, 22)

Coordinate switched back: -y direction now +z direction, again

Plasma injection occurs at z~18 cm in upstream (-z) direction

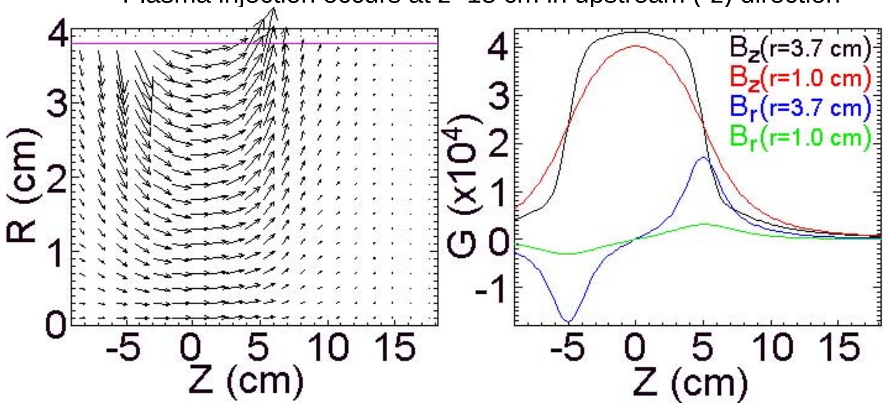


Coordinate switched back: -y direction now +z direction, again

Assumption (from reduced dimensionality):
$J_z^i$ ~ 0.3, 0.6, 1.2, 2.4 A $cm^{-2}$ with constant $n_p$ ~ $10^{12}$ $cm^{-3}$ at injection plane

**4 cases:**
$v_z^i$ = -1.5, -3, -6, -12 cm/$\mu$s
$T_i$ ~ 1 eV and $T_e$ ~ 5 eV
($M_i$ ~ 2.7, 5.5, 11, 22)

Plasma density isocontours

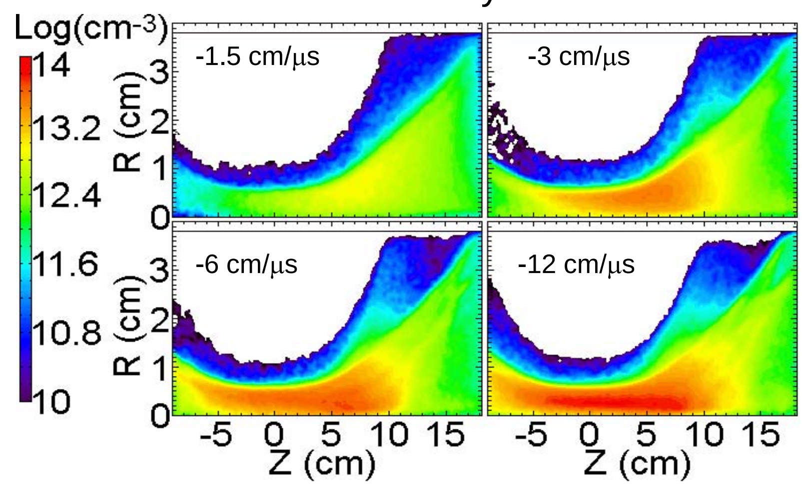

# 2D supersonic plasma injection into a 40 kG final-focus solenoid

Plasma injection occurs at z~18 cm in upstream (-z) direction

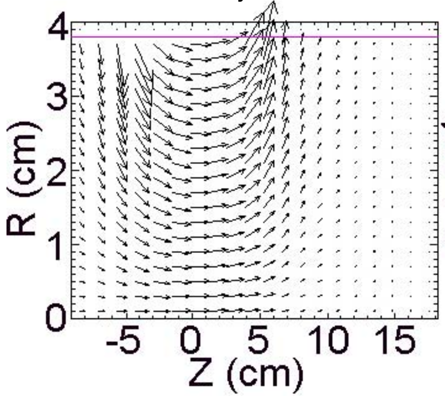


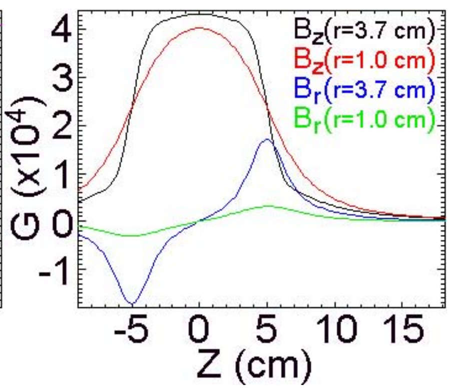


Assumption (from reduced dimensionality):
$J_z^i$ ~ 0.3, 0.6, 1.2, 2.4 A $cm^{-2}$ with constant
$n_p$ ~ $10^{12}$ $cm^{-3}$ at injection plane

**4 cases:**
$v_z^i$ = -1.5, -3, -6, -12 cm/μs
$T_i$ ~ 1 eV and $T_e$ ~ 5 eV
($M_i$ ~ 2.7, 5.5, 11, 22)

Coordinate switched back: -y direction now +z direction, again

Plasma density isocontours

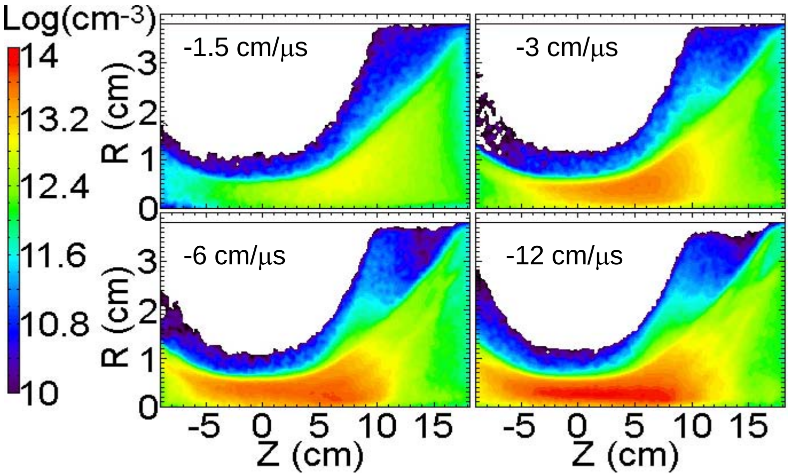


{z, vz} plasma ion phase space

-1.5 cm/μs

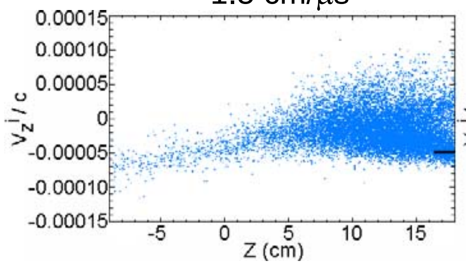


-12 cm/μs

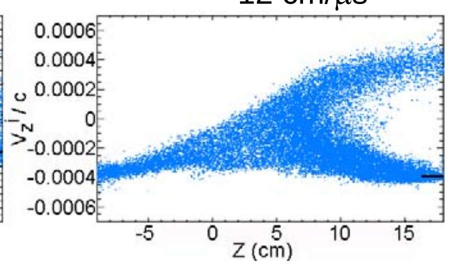


Counter-propagating streams: magnetic mirroring!

# Measured: high-density plasma penetration into $B_z$ = 40-50 kG solenoids 

**Poster tomorrow: P. K. Roy [ THPAS006 ]**

Compression of plasma measured

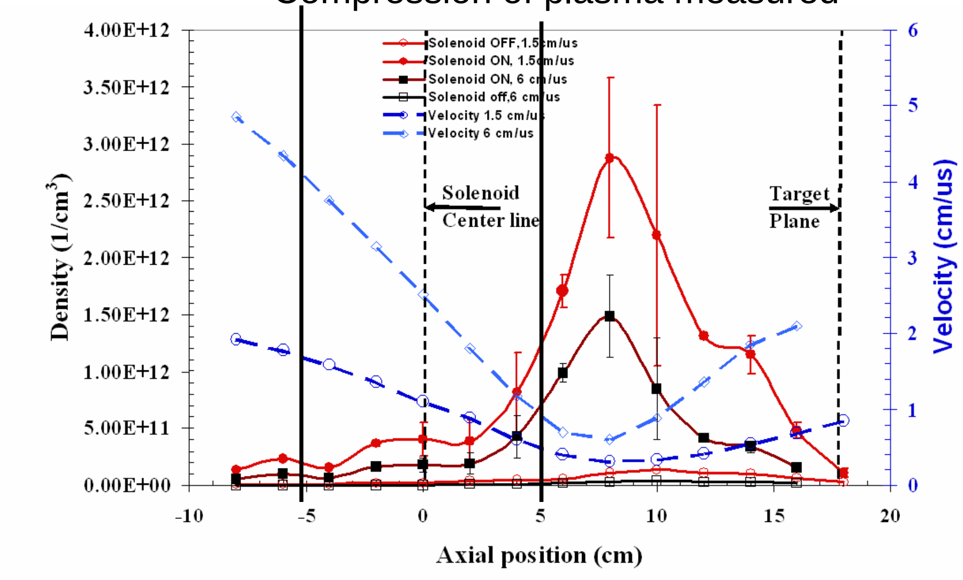

# Measured: high-density plasma penetration into $B_z$ = 40-50 kG solenoids



**Poster tomorrow: P. K. Roy [ THPAS006 ]**

Compression of plasma measured

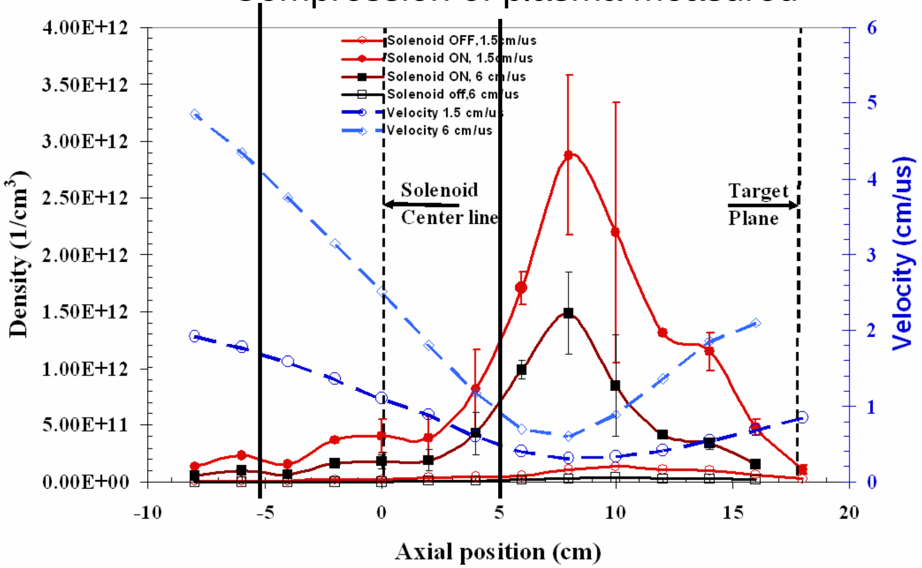


Preliminary experiment and simulation comparison

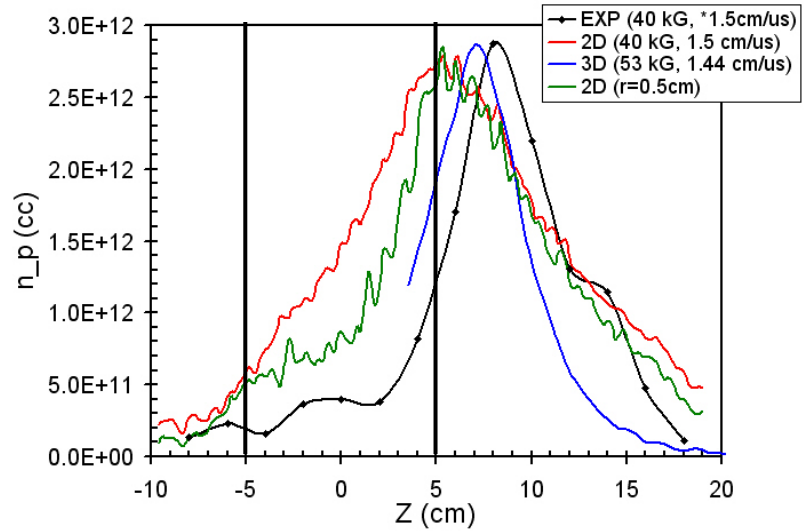

# Measured: high-density plasma penetration into $B_z$ = 40-50 kG solenoids 

**Poster tomorrow: P. K. Roy [ THPAS006 ]**

Compression of plasma measured

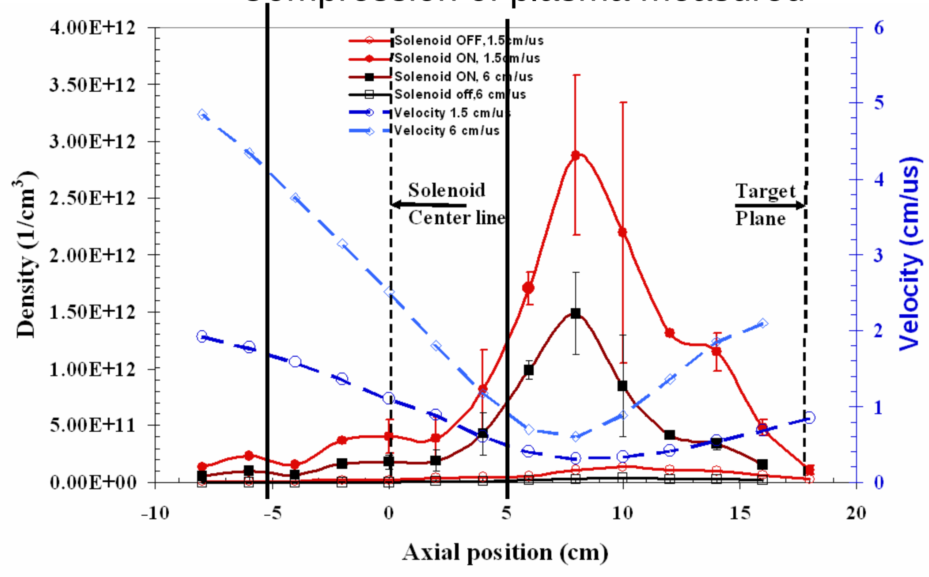


Preliminary experiment and simulation comparison

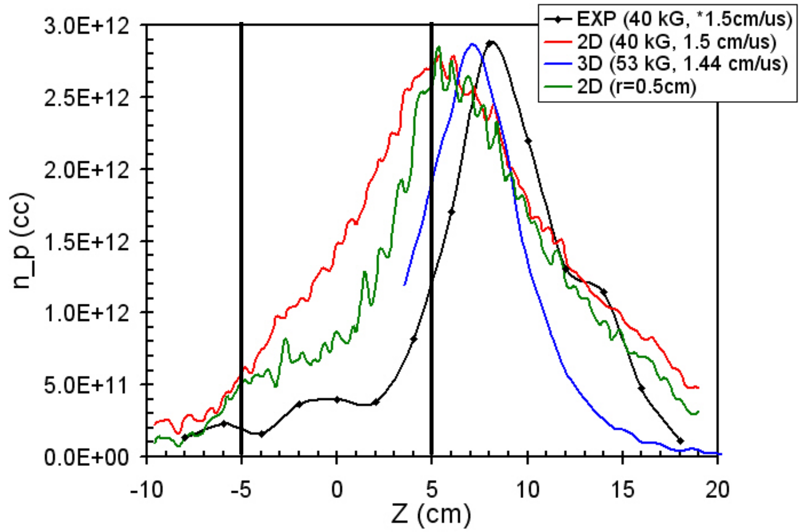


$n_p$ isocontours in presence of final-focus solenoid

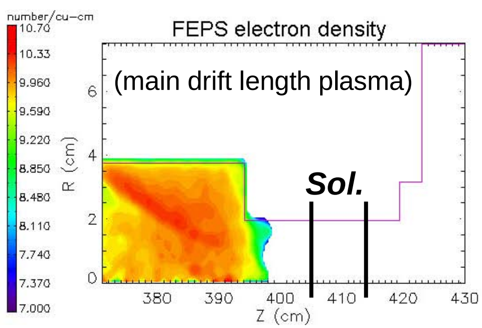


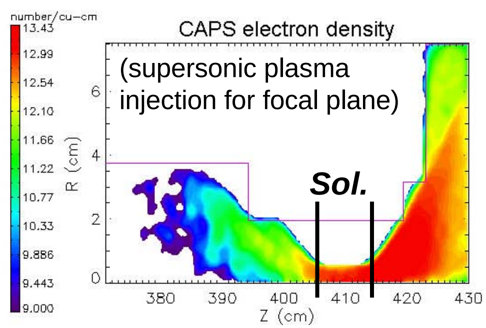

**Poster tomorrow: P. K. Roy [ THPAS006 ]**

## Compression of plasma measured

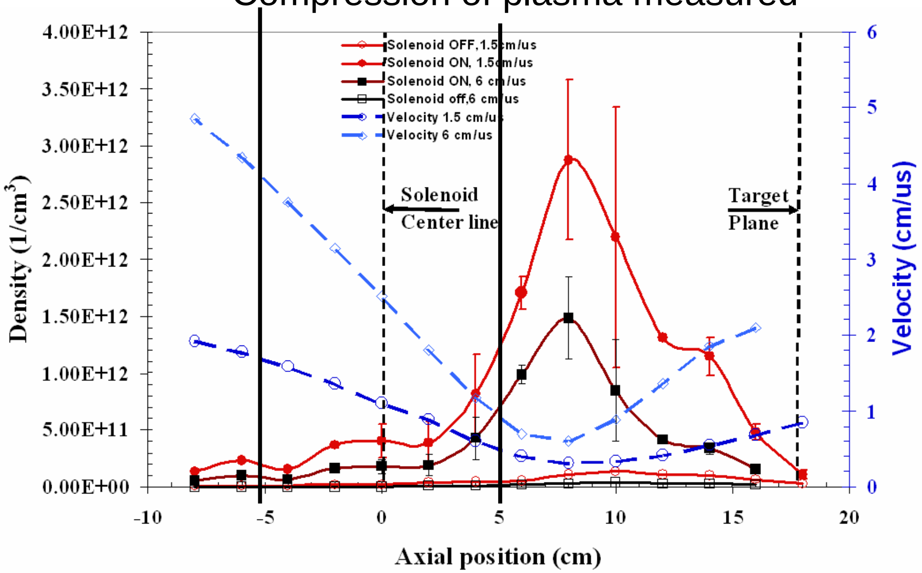


## Preliminary experiment and simulation comparison

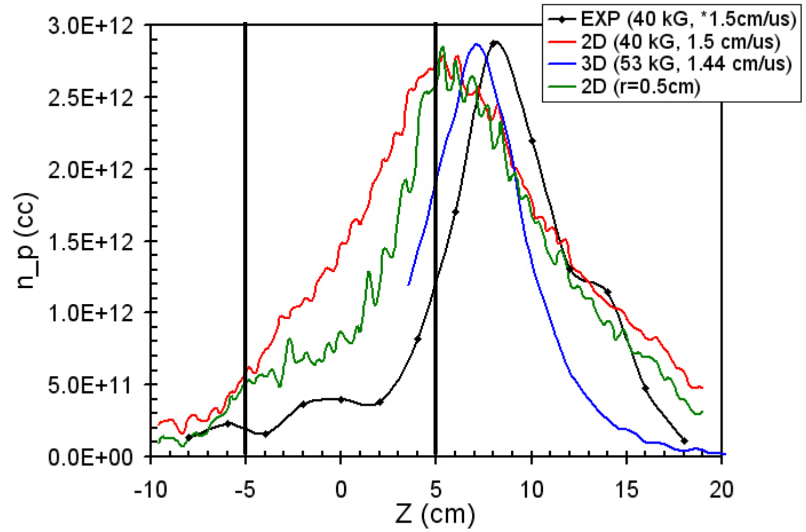


## $n_p$ isocontours in presence of final-focus solenoid

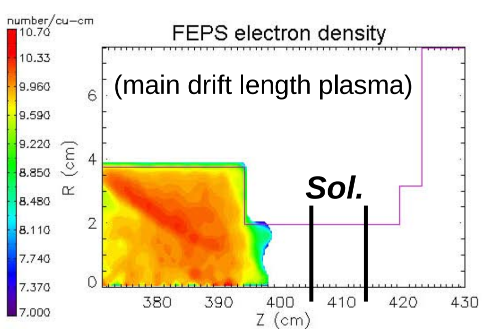


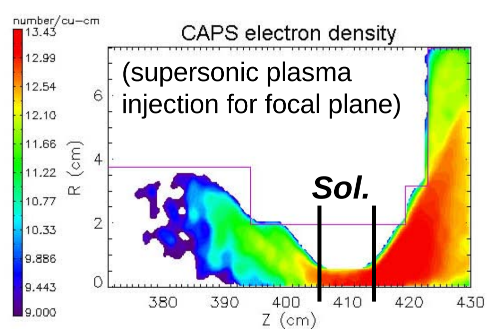


## Preliminary simultaneous compression comparison

Simulation, in presence of simulated “realistic” plasma profiles (left)

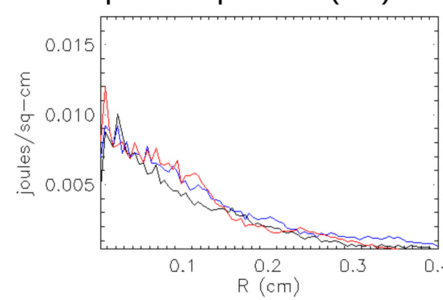


Experiment ($B_z$ ~ 50 kG)

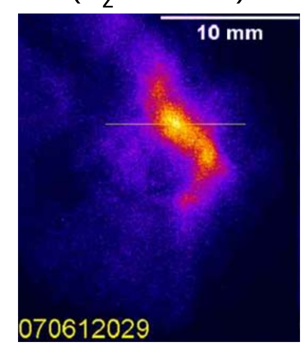

# Outline

0) MOTIVATION AND ISSUES
- a) Overview
- b) Plasma neutralization-assisted focusing of space-charge-dominated beams

1) LONGITUDINAL COMPRESSION: ACCELERATION GAP EFFECTS
- a) Finite-size gap and voltage waveform
- b) Non-zero initial beam temperature (emittance)
- c) Initial pulse length $t_p$, intended fractional tilt *f*, and initial beam energy
- d) Comparison: theoretical models, particle-in-cell simulation, and experiment

2) TIME-DEPENDENT TRANSVERSE DEFOCUSING EFFECT OF THE ACCELERATION GAP
- a) Description of the effect
- b) The "over-focusing" technique for simultaneous transverse and longitudinal compression

3) SIMULTANEOUS FOCUSING USING A STRONG FINAL-FOCUS SOLENOID
- a) Focal plane aberration due to static magnetic field and beam velocity tilt
- b) Supersonic cathodic-arc plasma injection into the high-field region from the low-field end
- c) Collective excitations during the beam-plasma interaction for $n_b > n_p$

# Peak energy deposition depends on plasma density (esp. near focal plane)

PIC simulations show the beam-plasma interaction during simultaneous compression in cases with $n_b < n_p$ and $n_b > n_p$ in a 150 kG solenoid.

PIC simulations show the beam-plasma interaction during simultaneous compression in cases with $n_b < n_p$ and $n_b > n_p$ in a 150 kG solenoid.

Higher $n_p$s are required in the presence of a strong **B** field ($c/\omega_{pe} >> \rho_{Le}$). The $L_b$ can decrease to $O(r_b)$ at focus [and $O(c/\omega_{pe})$] so that charge neutralization is harder to provide for a given amount of plasma.

PIC simulations show the beam-plasma interaction during simultaneous compression in cases with $n_b < n_p$ and $n_b > n_p$ in a 150 kG solenoid.

Higher $n_p$s are required in the presence of a strong **B** field ($c/\omega_{pe} >> \rho_{Le}$). The $L_b$ can decrease to $O(r_b)$ at focus [and $O(c/\omega_{pe})$] so that charge neutralization is harder to provide for a given amount of plasma.

Cumulative energy deposition profiles through the intended simultaneous focal plane

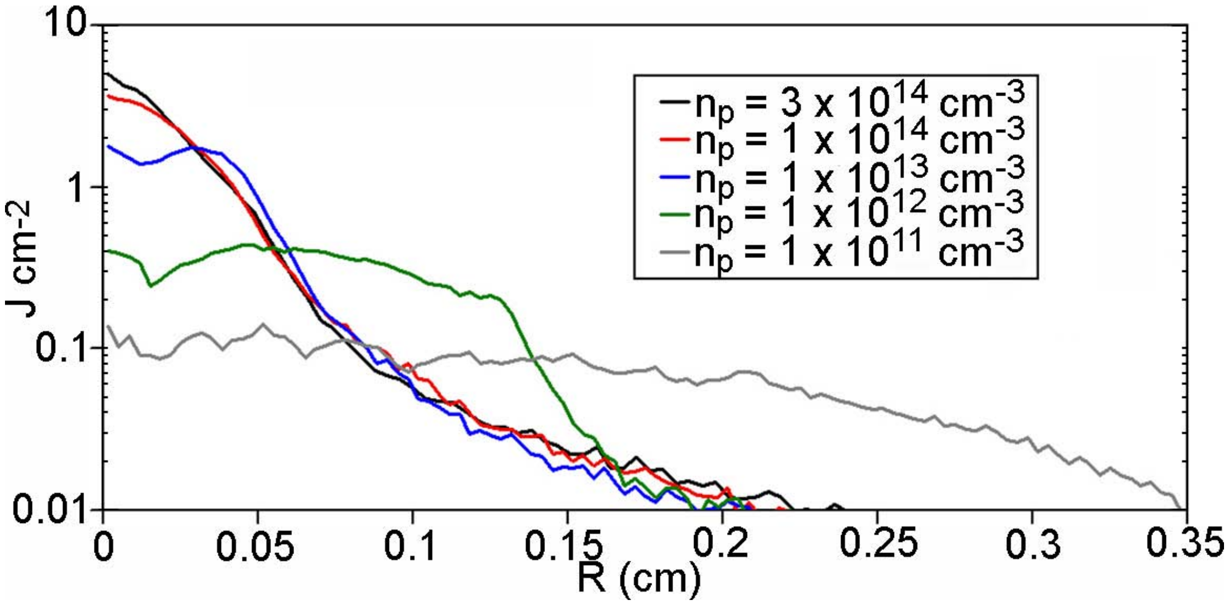

# Charge and current quasi-neutrality lost when $n_b > n_p$



The $n_b$ can approach the $n_p$, *especially near the focal plane*, and the assumption of charge and current neutralization may become invalid, leading to large perturbations in the plasma and field properties.

*Strong final-focus solenoid present here, cold background carbon plasma modeled*

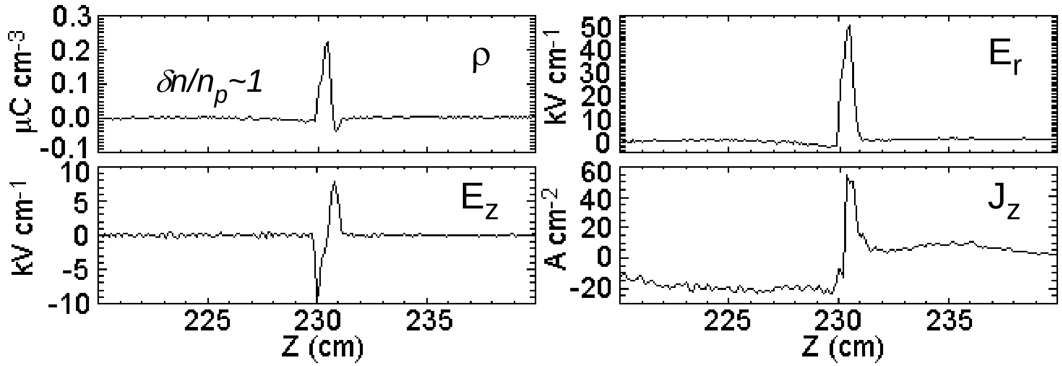

# Charge and current quasi-neutrality lost when $n_b > n_p$



The $n_b$ can approach the $n_p$, *especially near the focal plane*, and the assumption of charge and current neutralization may become invalid, leading to large perturbations in the plasma and field properties.

*Strong final-focus solenoid present here, cold background carbon plasma modeled*

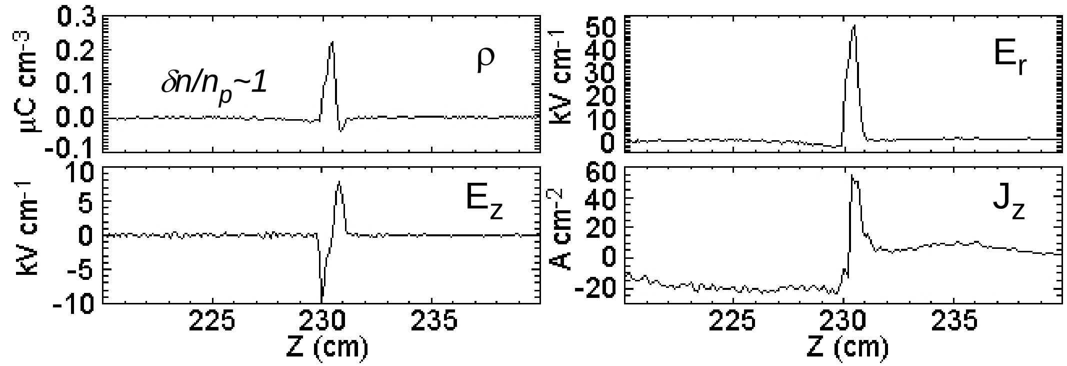


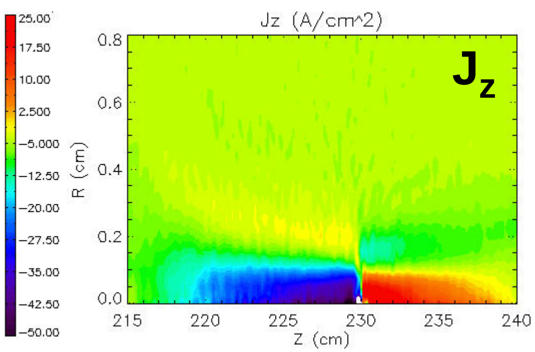


As the beam tries to focus with $n_b > n_p$,
(1) LEFT: the $\rho$ and **J** will become increasingly unneutralized,
(2) BOTTOM: the defocusing self-fields of the beam will grow, and
(3) RIGHT: the plasma will locally heat.

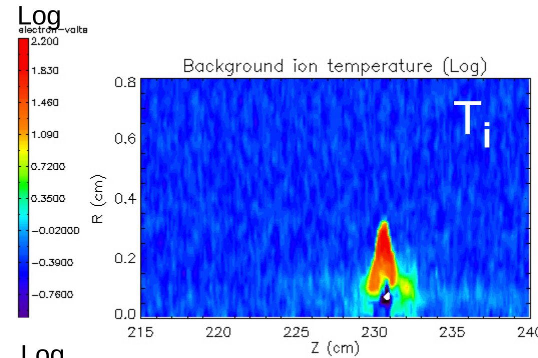


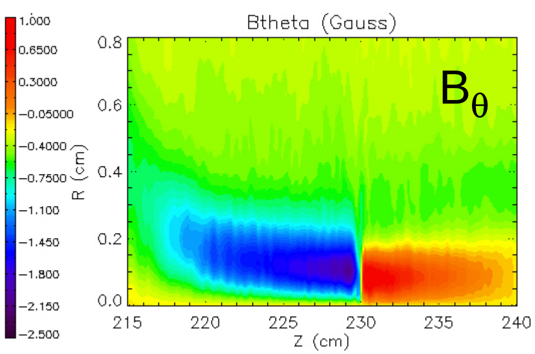


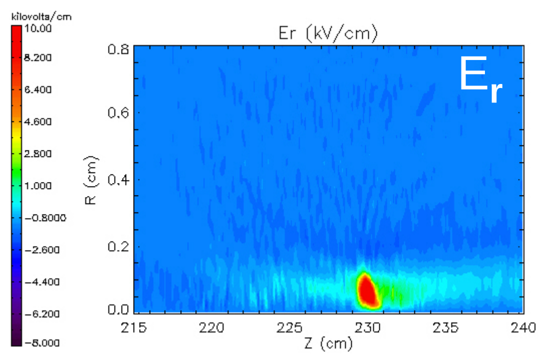


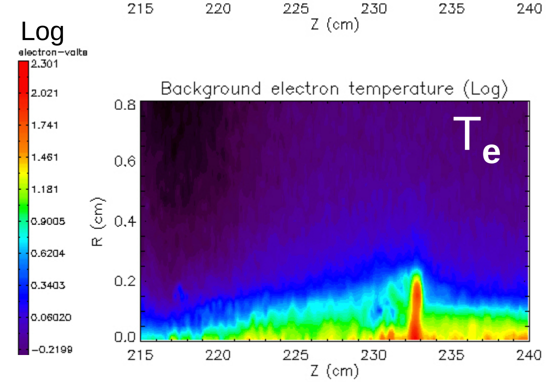

Once the beam stagnates, the plasma supports strong electrostatic and electromagnetic excitations, due to large perturbations created during stagnation of the ion beam.

Snapshots at t = +55 ns after stagnation

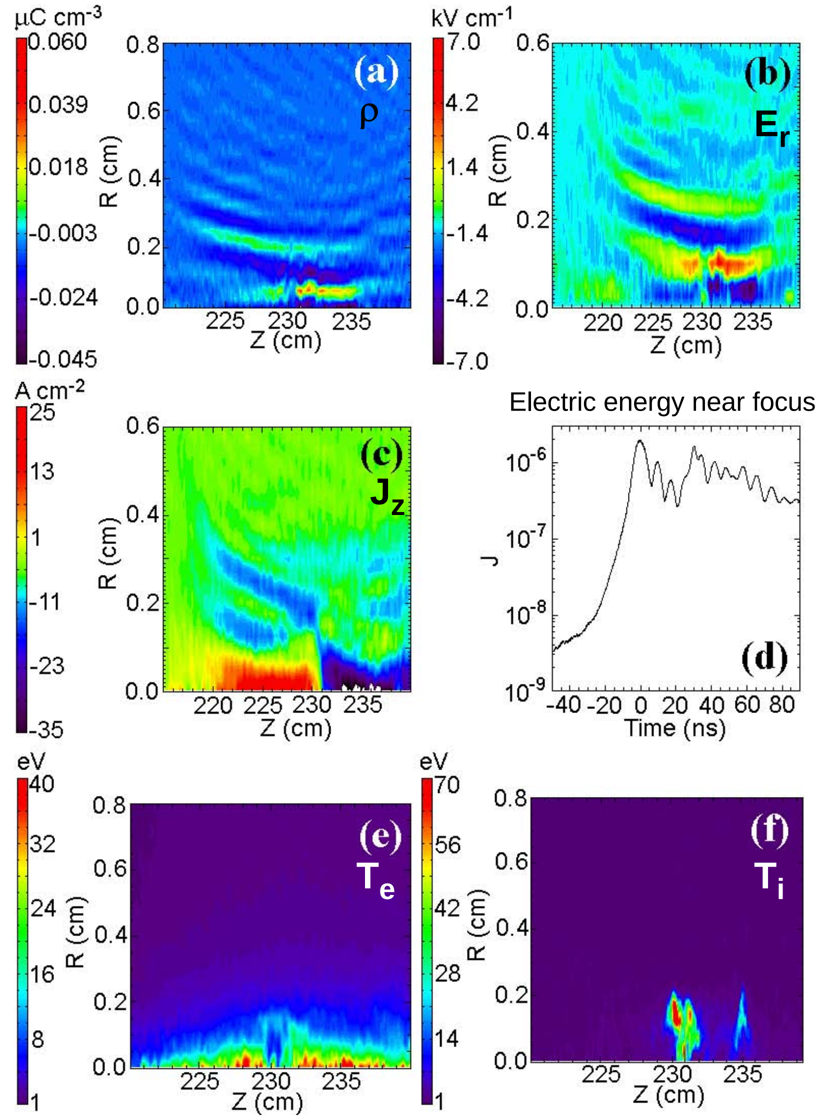


*A. B. Sefkow, *et al.*, *Nucl. Instrum. Meth. Phys. Res. A* **577**, 288 (2007).

# Plasma responds to beam's self-fields with collective excitations*

Once the beam stagnates, the plasma supports strong electrostatic and electromagnetic excitations, due to large perturbations created during stagnation of the ion beam.

Observed frequency: $\omega \sim 8 \times 10^8$ rad s$^{-1}$
Range: $[\Omega_{ci} < \omega_{pi} < \omega << \omega_{pe} < \Omega_{ce}]$
Carbon plasma: $m_e / m_i \sim 4.5 \times 10^{-5}$
k $\perp \mathbf{B}_{sol}$ with $k_\perp \sim 6.3 \times 10^3$ m$^{-1}$, with a small component satisfying $k_\parallel / k_\perp \sim 4 \times 10^{-3}$.

Electrostatic lower hybrid oscillation:
$$\omega^2 \sim \tfrac{1}{2}(\omega_{pe}^2+\Omega_{ce}^2) - \tfrac{1}{2}[(\omega_{pe}^2+\Omega_{ce}^2)^2 - 4\omega_{pe}^2\, \Omega_{ce}^2 \cos^2\theta]^{1/2}$$

Snapshots at t = +55 ns after stagnation

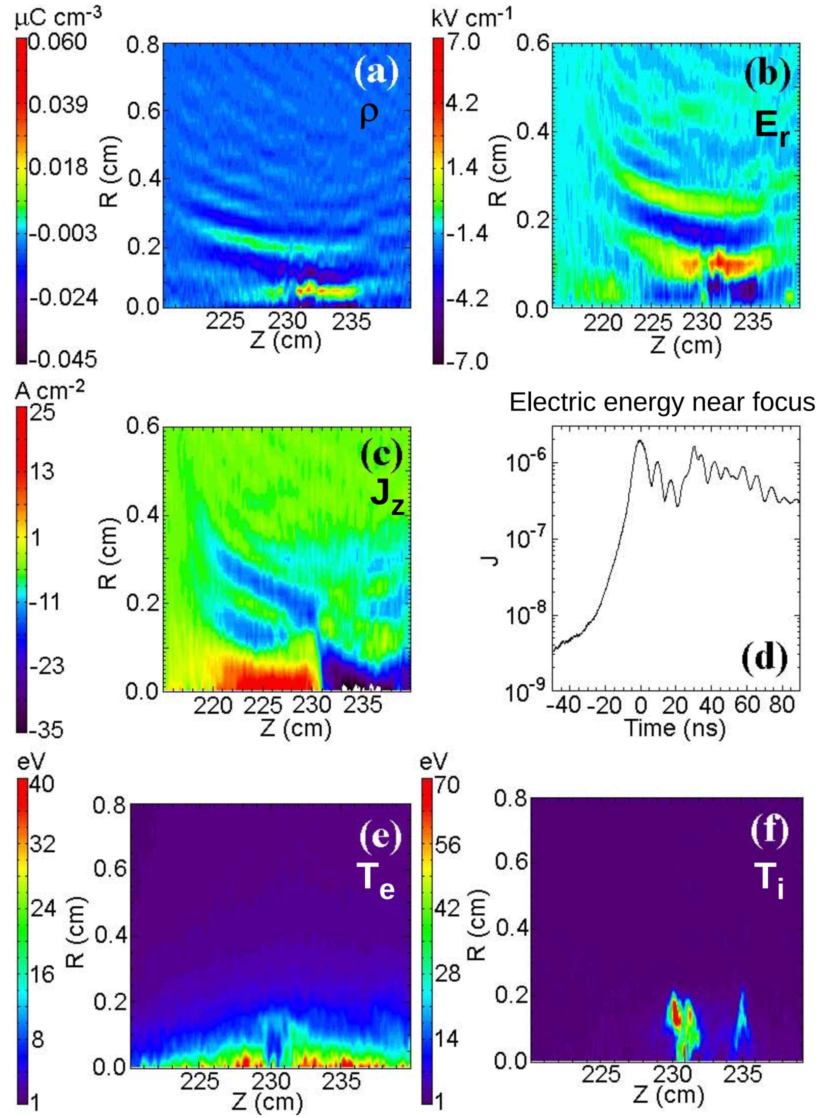


Plasma densities t = +33 ns after stagnation
($n_{p0} \sim 10^{12}$ cm$^{-3}$)

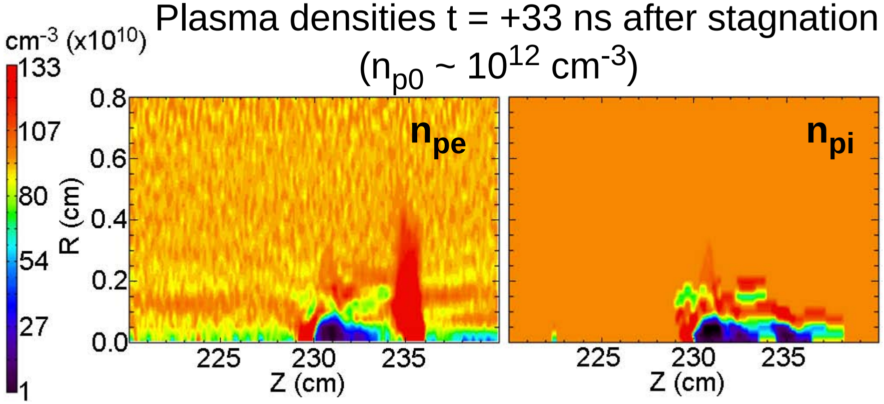


*A. B. Sefkow, *et al.*, *Nucl. Instrum. Meth. Phys. Res. A* **577**, 288 (2007).

1. In order to achieve high intensities on target with space-charge-dominated beams, plasma neutralization-assisted focusing is required.

# Summary and conclusions

1. In order to achieve high intensities on target with space-charge-dominated beams, plasma neutralization-assisted focusing is required.

2. Longitudinal bunch compression in the laboratory is constrained by acceleration gap size, voltage waveform shape and accuracy, beam temperature, initial pulse length, intended fractional tilt, and energy accuracy for the specified waveform. Excellent agreement is found between theory, simulations, and recent experimental measurements.

1. In order to achieve high intensities on target with space-charge-dominated beams, plasma neutralization-assisted focusing is required.

2. Longitudinal bunch compression in the laboratory is constrained by acceleration gap size, voltage waveform shape and accuracy, beam temperature, initial pulse length, intended fractional tilt, and energy accuracy for the specified waveform. Excellent agreement is found between theory, simulations, and recent experimental measurements.

3. The “over-focusing” technique may be used to recover mm spot sizes by offsetting the time-dependent transverse defocusing effect, which is an inherent side-effect of the longitudinal focusing process.

# Summary and conclusions

1. In order to achieve high intensities on target with space-charge-dominated beams, plasma neutralization-assisted focusing is required.

2. Longitudinal bunch compression in the laboratory is constrained by acceleration gap size, voltage waveform shape and accuracy, beam temperature, initial pulse length, intended fractional tilt, and energy accuracy for the specified waveform. Excellent agreement is found between theory, simulations, and recent experimental measurements.

3. The “over-focusing” technique may be used to recover mm spot sizes by offsetting the time-dependent transverse defocusing effect, which is an inherent side-effect of the longitudinal focusing process.

4. Simulations show current density compression by factors from $10^3$ to over $10^6$, depending on the strength and focal length of the focusing elements. Final-focus solenoids can be used for extreme simultaneous compression, and high-density supersonic plasma has been simulated and measured to partially penetrate strong solenoids for beam neutralization purposes.

1. In order to achieve high intensities on target with space-charge-dominated beams, plasma neutralization-assisted focusing is required.

2. Longitudinal bunch compression in the laboratory is constrained by acceleration gap size, voltage waveform shape and accuracy, beam temperature, initial pulse length, intended fractional tilt, and energy accuracy for the specified waveform. Excellent agreement is found between theory, simulations, and recent experimental measurements.

3. The “over-focusing” technique may be used to recover mm spot sizes by offsetting the time-dependent transverse defocusing effect, which is an inherent side-effect of the longitudinal focusing process.

4. Simulations show current density compression by factors from $10^3$ to over $10^6$, depending on the strength and focal length of the focusing elements. Final-focus solenoids can be used for extreme simultaneous compression, and high-density supersonic plasma has been simulated and measured to partially penetrate strong solenoids for beam neutralization purposes.

5. Beam-plasma interaction simulations near the simultaneous focal plane illustrate compression stagnation for $n_{beam} > n_{plasma}$ and that the plasma supports collective excitations in the background plasma with an external B field.

The **physics foundation** of <u>simultaneous transverse and longitudinal focusing of intense charge bunches</u> in

*the Neutralized Drift Compression eXperiment (NDCX)*

will provide key insights for the next-step heavy ion beam experiments. The ultimate goal is the development of heavy ion drivers for warm-dense-matter, high-energy-density, and heavy ion fusion applications.